AD A103106

(12) LEVEL II

NRL Memorandum Report 4598

Excitation and Ionization Cross Sections for Electron Beam and Microwave Energy Deposition in Air

A. W. Ali

Plasma Physics Division

DTIC
ELECTE
AUG 20 1981
S D
B

August 20, 1981

This report was sponsored by Advanced Research Projects Agency (DoD), ARPA Order No. 3718, monitored by C.M. Huddleston under Contract #N60921-80-WR-W0190 and Naval Air Systems Command 62734N-80-WF34-388-501.

NAVAL RESEARCH LABORATORY
Washington, D.C.

Approved for public release; distribution unlimited.

81 8 19 104

DTIC FILE COPY

(9) Memorandum Rept.

SECURITY CLASSIFICATION OF THIS PAGE (When Data Entered)

(14) REPORT DOCUMENTATION PAGE

READ INSTRUCTIONS BEFORE COMPLETING FORM

1. REPORT NUMBER: NRL Memorandum Report 4598 (NRL-MR-)
2. GOVT ACCESSION NO.: AD-A103 196
3. RECIPIENT'S CATALOG NUMBER:

(6) 4. TITLE (and Subtitle): EXCITATION AND IONIZATION CROSS SECTIONS FOR ELECTRON BEAM AND MICROWAVE ENERGY DEPOSITION IN AIR

5. TYPE OF REPORT & PERIOD COVERED: Interim report on a continuing NRL problem.

6. PERFORMING ORG. REPORT NUMBER:

(10) 7. AUTHOR(s): A. W. Ali

(11) 20 Aug 81

8. CONTRACT OR GRANT NUMBER(s): (15) ARPA Order 3718

9. PERFORMING ORGANIZATION NAME AND ADDRESS: Naval Research Laboratory, Washington, DC 20375 (12) 55

10. PROGRAM ELEMENT, PROJECT, TASK AREA & WORK UNIT NUMBERS: 61101E; 47-0900-00

11. CONTROLLING OFFICE NAME AND ADDRESS: Defense Advanced Research Projects Agency, Arlington, VA 22209; Naval Air Systems Command, Washington, DC 20361

12. REPORT DATE: August 20, 1981

13. NUMBER OF PAGES: 52

14. MONITORING AGENCY NAME & ADDRESS (if different from Controlling Office): Naval Surface Weapons Center, Silver Spring, MD 20910

15. SECURITY CLASS. (of this report): UNCLASSIFIED

15a. DECLASSIFICATION/DOWNGRADING SCHEDULE:

16. DISTRIBUTION STATEMENT (of this Report)

Approved for public release; distribution unlimited.

(16) F34388

17. DISTRIBUTION STATEMENT (of the abstract entered in Block 20, if different from Report)

(17) WF34388501

18. SUPPLEMENTARY NOTES

This report was sponsored by Advanced Research Projects Agency (DoD), ARPA Order No. 3718, monitored by C.M. Huddleston under Contract #N60921-80-WR-W0190 and Naval Air Systems Command 62734N-80-WF34-388-501.

19. KEY WORDS (Continue on reverse side if necessary and identify by block number)

N_2
O_2
Excitation
Ionization
Cross sections

20. ABSTRACT (Continue on reverse side if necessary and identify by block number)

A set of excitation and ionization cross sections for electron collisions in N_2, O_2, N and O are presented.

DD FORM 1 JAN 73 1473 EDITION OF 1 NOV 65 IS OBSOLETE
S/N 0102-014-6601

SECURITY CLASSIFICATION OF THIS PAGE (When Data Entered)

251950

CONTENTS

1. INTRODUCTION 1

2. NITROGEN MOLECULE 1

2.1 Vibrational Excitation Cross Section 1
2.2 N_2-Triplet States 2
2.3 N_2-Singlet States 4
2.4 Higher Level Singlets and Triplets 6
2.5 The Dissociation Cross Section of N_2 6
2.6 Ionization and Dissociative Ionization Cross Sections of N_2 7

3. OXYGEN MOLECULE 8

3.1 Vibrational Excitation Cross Section O_2 8
3.2 $a^1\Delta$ and $b^1\Sigma$ States of O_2 8
3.3 $A^3\Sigma$ 9
3.4 $B^3\Sigma$ 9
3.5 The Ionization and Dissociative Ionization of O_2 9

4. OXYGEN ATOM 10

4.1 Oxygen Atom Low Lying Metastable States $O(^1D)$ and $O(^1S)$ 10
4.2 Optically Allowed Transitions 10
4.3 Ionization Cross Section of O 11

5. NITROGEN ATOM 12

5.1 Low Lying Metastable States $N(^2D)$ and $N(^2P)$ 12
5.2 Optically Allowed Transitions 12
5.3 Ionization Cross Section of Nitrogen Atoms 12

REFERENCES 43

DTIC
ELECTE
AUG 20 1981
S D
B

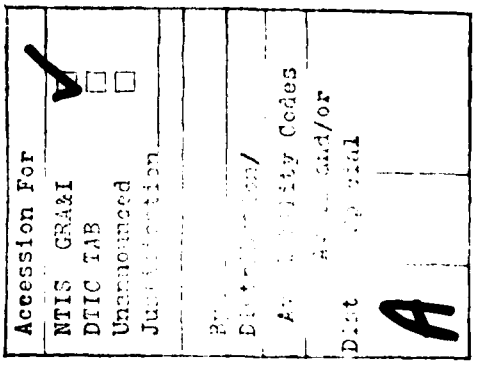

EXCITATION AND IONIZATION CROSS SECTIONS FOR ELECTRON BEAM AND MICROWAVE ENERGY DEPOSITION IN AIR

1. Introduction

The electron energy deposition in air, or any other gaseous element, requires a detailed consideration of all elastic and inelastic electron-atom and electron-molecule interactions. The inelastic processes include the excitation, dissociation and ionization of the air species. Electron excitation of molecules, however, are rotational, vibrational and electronic in nature. The elastic processes, on the other hand, constitute the electron neutral and the electron ion momentum transfer collisions.

Each collision process, by an electron with an air species, is characterized by a cross section. This cross section has to be known, experimentally or theoretically, over a wide energy range of the incident electron. The wide energy range, for the cross section, from excitation threshold to infinity, is required in order to account for the energy deposition of highly energetic electrons (the incident primary) and the generated secondaries and tertiaries, down to the thermal electrons. However, the low energy behaviour of the cross section from threshold to few times beyond threshold is also essential for the microwave energy deposition in air.

In this report we present a set of cross sections for the electron collisions with N_2, O_2, O and N. Data on these cross sections were reported[1] previously. However, some have changed drastically, while new data have become available where none existed before. Furthermore, disagreement exists on the shape and the peak value of the cross section when there is more than one source for the data, as can be seen in this report.

2. Nitrogen Molecule

2.1 Vibrational Excitation Cross Section

The electron impact excitation cross section for eight ground state vibrational levels of the nitrogen molecule have been measured by

Manuscript submitted June 29, 1981.

Schulz[2] and Ehrhardt and Willman[3]. Theoretical calculations have been carried[4-6] out with satisfactory reproduction of the experimental results.[6] The measured cross sections of Schulz[2] are shown in Figures 1 - 8 for the individual vibrational levels adjusted[7] to a peak value of $6.0 \times 10^{-16} cm^2$ at 2.5 eV for the total vibrational excitation cross section, which is in good agreement with a previously predicted[8] value.

2.2 N_2-Triplet States

$A^3\Sigma$: The electron impact excitation cross section of $A^3\Sigma$ state from the ground state of N_2, has been calculated[9,10] and measured[11-13] by several investigators. These results are shown in Fig. 9 except for Cartwright's earlier calculation[9] which is larger by a factor of $\sim$1.6 compared to the calculations of Chung and Lin.[10] The most recent measurement by Cartwright, et al,[13] however, has the lowest value for the peak cross section compared to other measurements.[11,12] Furthermore, the peak of the cross section occurs at an electron energy of $\sim$17 eV compared to $\sim$11 eV for measurements of Brinkman and Trajmar[11] and Borst.[12] The theoretical calculation of Chung and Lin[10] also predict the peak cross section to occur at 11 eV.

The best choice for the cross section, in our view, is that of Borst,[12] provided the peak of the cross section is adjusted to the recent value of Cartwright, et al[13] to eliminate the effect of cascade contribution from higher levels. The lowest electron energy, for which cross section data is available, is 8 eV. The extension of the cross section downward to the threshold, which is at 6.17 eV, is indicated by a dashed line (See Fig. 9). For electron energies above 40 eV, the cross section data can be obtained using the $\frac{1}{E^3}$ dependence[14,15] of the cross section on the electron energy.

$B^3\Pi$: The electron impact excitation of the $B^3\Pi$ state from the ground state of N_2, has been measured by Cartwright, et al[13] and Brinckman and Trajmar[11] and calculated by Cartwright[9] and Chung and Lin[10].

As seen from Figure 10, there is good agreement between the theoretical[10] and the recently measured[13] cross section except for their behaviour at electron energies above 30 eV. The theoretical cross section of Cartwright[9] is not shown in Figure 10. However its peak value is $\sim 3.1 \times 10^{-17}$ cm^2 and occurs at $\sim$ 17 eV.

For electron energies above 30 eV the cross section data can be obtained using the $\frac{1}{E^3}$ dependence[14,15] of the cross section on the electron energy. At the low energy, data is available at 8 eV. This could be extended downward to zero at threshold, which is at 7.4 eV.

$C^3\Pi$: The electron impact cross section for the excitation of the $C^3\Pi$ state, from the ground state of N_2, has been measured[11,13] and calculated.[9,10] There is good agreement between the theoretical values[9,10] as well as the experimental[11,13] data as seen in Fig. 11. The theoretical cross section of Cartwright[9] is not shown. However, its peak value is $\sim 4.4 \times 10^{-17}$ cm^2 and occurs at $\sim$ 15 eV.

The high energy behaviour of the cross section can be obtained by utilizing the energy dependence of the (0,0) emission at 3371Å, also shown in Fig. 11, as measured by Imami and Borst[16]. The energy dependence of the cross section follows an $E^{-2.2}$ rather than the expected $E^{-3.0}$ dependence. The absolute cross section for the (0,0) emission can be converted into an absolute cross section for the total excitation of $C^3\Pi$ state by multiplying the emission cross section by a factor of 3.55, where the appropriate Franck Condon factors are utilized. This brings the peak cross section to 3.9×10^{-17} cm^2 which is in good agreement with measurements of Cartwright, et al[13] and Brinckman and Tragman[11]. The best choice would be

the latest measured cross section[13] with the utilization of the $E^{-2.2}$ dependence for the cross section above 50 eV. For low energy, the data at 12 eV can be extended downward to zero at threshold, which is at 11.0 eV.

$W^3\Delta$: The electron impact excitation cross section of $W^3\Delta$ state from the ground state of N_2 has been measured[13] and calculated[10]. However, the experimental value is higher by a factor of 5 compared to the calculated value at the peak. Furthermore, the shape of the theoretical cross section differs variedly from the measured shape. We opt for the experimental data which has an expected shape for a singlet to triplet excitation. The high energy value should follow a $E^{-3.0}$ dependence[14,15]. The low energy portion can be obtained by extending the value at 8 eV downward to zero at threshold, which is at 7.36 eV.

$B'^3\Sigma$: The electron impact excitation cross section of $B'^3\Sigma$ from the ground state of N_2 has been measured by Cartwright et al.[13] No other data is available. The high energy behaviour can be scaled with an $E^{-3.0}$ dependence. For the low energy portion, data is available at 9 eV and can be scaled downward to zero at threshold, which is at 8.2 eV.

$E^3\Sigma$: The electron impact excitation cross section of the $E^3\Sigma$ state from the ground state of N_2 has been calculated[9,10] and measured[13]. However, the agreement is not good. The theoretical cross sections of Cartwright[9] and Chung and Lin[10] yield peak values of $1.7 \times 10^{-17} cm^2$, $3.7 \times 10^{-18} cm^2$, respectively. The recent measurement[13], on the other hand, has a peak value of $\sim 0.80 \times 10^{-18} cm^2$ and is shown in Fig. 14. The excitation threshold for the $E^3\Sigma$ is 11.9 eV.

2.3 N_2 Singlet States

$a'^1\Sigma$: The electronic impact excitation cross section of $a'^1\Sigma$ state from the ground state of N_2 has recently been measured[13] and is shown in

Fig. 15. The high energy behaviour can be scaled from the present data with a $\frac{1}{E}$ dependence.

$a^1\Pi$: The electron impact excitation of the $a^1\Pi$ state from the ground state of N_2 has been calculated[10] and measured[11,12,13,19,20] extensively. There seems to be a reasonable agreement on the shape of the measured cross sections. Measurements of Borst[12] and Fin and Doering[19] are in excellent agreement. They are higher by ∿25% compared to the recent measurement of Cartwright, et al.[13] These cross sections are shown in Fig. 16 for comparison. Ajell's[20] cross section is not shown; however, it is in good agreement with that of Finn and Doering[19] from threshold to an electron energy of ∿20 eV. Beyond 20 eV, however, it falls off slower with energy compared to that of Finn and Doering.[19] The latest measurement[13] is preferred for modeling purposes and data above 50 eV is to obtained by scaling the cross section with a E^{-1} dependence. On the other hand, for lower energy the cross section can be obtained by scaling data at the lowest energy to zero at threshold, which is at 8.5 eV.

$w^1\Delta$: The electron impact excitation cross section of $w^1\Delta$ state from the ground state of N_2 has been calculated[10] and measured[13]. The agreement between the calculated and the measured cross section is very poor. The recent measured[13] value, however, as shown in Fig. 17 is preferred. The high energy behaviour should follow an E^{-1} dependence. The energy data can be estimated by scaling the data at the lowest energy to zero at threshold, which is at 8.9 eV.

$a'' {}^1\Sigma$: The electron impact excitation cross section of $a'' {}^1\Sigma$ state has been measured[13] and calculated[10]. However, the agreement is very poor in the shape, where the peak occurs, and the high energy behaviour. The experimental[13] cross section should be preferred. For high energy the σ is to be scaled with E^{-1} dependence. For low energy, the data at the lowest

energy is to be scaled downward to zero at threshold, which is at 12.3 eV.

2.4 Higher level singlets and triplets

Higher lying singlet and triplet cross sections in the electron energy range of 12.5 - 14.2 have beam measured by Chutjian, et al[21], however, most of the singlet states contribute to the dissociation of N_2 through their predissociation (See Section 2.5) and will not be given here. However the cross sections for two triplet states, $F^3\pi$ and $G^3\pi$ and two triplet-like states, designated M_1 and M_2 by Chutjian et al[21], are shown in Fig. 19.

2.5 The Dissociation Cross Section of N_2

The total dissociation cross section of N_2 by electron impact was first measured by Winters[22] for electron energies up to 300 eV. This total cross section is the sum of two distinct processes which have different threshold energies. These processes are the pure dissociation of N_2 where the atoms are either in their ground state or in an excited state (Dissociative Excitation), and the dissociative ionization. The dissociative ionization can result in the products of the dissociation to be either in their ground states or in an excited state. The simple dissociation of N_2 can be obtained from the total dissociation cross section by subtracting the contribution of the dissociative ionization.

Recently, Zipf and McLaughlin[23] have analysed the electron impact dissociation in considerable detail, delineating the contribution of various excited states towards the total dissociation of N_2. The total dissociation cross section analysed in this manner is in good agreement with measured cross sections of Winters[22] and Niehaus.[23]

In the analysis of Zipf and McLaughlin[23], it is shown that the N_2 singlet states in the energy range of 12.5 to 14.9 eV account for 60% of the total dissociation cross section, through their predissociations. Therefore, it is not necessary to provide additional individual cross

sections for N_2 singlets, e.g. $b'\Sigma$, $'\pi_u$, etc. Data is available on this if desired.

The total cross section for the dissociation of N_2 is shown in Figure 20. Also shown in this figure are the electron impact dissociative excitations which result in vacuum ultraviolet emissions from the nitrogen atom. Data from various references[25-28] are utilized to construct these emission cross sections.

2.6 Ionization and Dissociative Ionization Cross Sections of N_2

The total electron impact ionization cross section for N_2 has been measured by Rapp and Golden[29] and Tate and Smith[30] for electron energies from threshold to 1000 eV. The dissociative ionization has also been measured[31] in the same electron energy range. The data for ionization[29] and dissociative ionization[31] are shown in Figure 21. A recent measurement[32] of the dissociative ionization cross section for electron energies of 30 - 60 eV is also shown in Fig. 21 where at 60 eV the new data is ∿50% higher than that of Rapp et al.[31]

The ionization cross section measurements have been extended to an electron energy of 20,000 eV by Schram, et al.[33] This data overlaps with measurements of Rapp and Englander-Golden[28] in the energy range of 600-1000 eV and is lower by ∿ 20%. A measurement[34] for the ionization cross section exists at an electron energy of 1.5 MeV. The extension of Rapp and Englander-Golden data to higher energies is shown in Figure 22 where data from Schram, et al.[33] normalized to Rapp and Englander -Golden[29], is utilized. For still higher energies one must consider relativistic and polarization effects where the cross section becomes almost constant.

The partial ionization cross sections leading to various ionization continuua of N_2 i.e., X, A, B states of N_2^+ are also shown in Fig. 21.

Data at 21 eV and 100 eV are utilized[32,35,36] to construct these cross sections. At 21 eV, the distribution[32] of the X, A and B states are 0.36 0.56 and 0.08 of the total ionization cross section, respectively. At 100 eV, the absolute emission cross section[35] of the (0.0) band of the first negative system and the total[36] cross section of the A-state are utilized with the total and dissociative ionization cross sections to obtain the partial ionization cross section.

For higher electron energies the percent contributions of the various states at 100 eV is utilized. These cross sections and the pure dissociation cross section of N_2 are also shown in Fig. 22.

3. Oxygen Molecule

3.1 Vibrational Excitation Cross Section O_2

The electron impact excitation of O_2 was measured by Spence and Schulz[37]. However, the measurements indicated that the cross sections were small with peak values of $\sim 10^{-19}$ cm^2 for the excitation of V=1 and V=2 states. Linder and Schmidt[38], however, have obtained cross sections for the same levels which are larger by approximately two orders of magnitude. The individual cross sections are very narrow and are shown in Fig. 23.

3.2 $a^1\Delta$ and $b^1\Sigma$ States of O_2

The electron impact excitation cross sections of $a^1\Delta$ and $b^1\Sigma$ states of O_2 (forbidden transitions) have been measured for electron energy in the range of 2-4 eV by Lindner and Schmidt[38] and in the range of 5-50 eV by Trajmar, et al.[39,40] and from 20 - 200 eV by Wakiya,[41] Julienne and Krauss[42] have calculated the electron impact excitation cross section for $a^1\Delta$ using Born approximation. However, the agreement between theory and experiment near threshold is poor, as would be expected. On the other hand, the agreement is very good in the energy range of 20 - 50 eV. Cross

sections for $a^1\Delta$ and $b^1\Sigma$ based on measured values is presented in Fig. 24. For higher energies the cross sections can be scaled with energy dependence[41] of $E^{-2.7}$ and $E^{-2.9}$ for $^1\Delta$ and $^1\Sigma$, respectively.

3.3 $A^3\Sigma$

The electron impact excitation of three electronic states, $A^3\Sigma$, $C^3\Delta$ and $C^1\Sigma$ (Forbidden Transitions) from the ground state of O_2, have been measured by Wakiya[41] for electron energy range of 20-500 eV and by Trajmar, et al.[40] at 20 and 40 eV. Wakiya's data are presented in Fig. 25. The cross section below 20 eV, shown as a dashed line in Fig. 25, is obtained using the theoretical expression given by Green and Stolarski,[43] normalized to experimental data at 20 eV. For electron energies above 300 eV the cross section can be scaled with an energy dependence[41] of E^{-1}. The excitation cross section for $A^3\Sigma$ is to be utilized as a dissociation cross section resulting in two oxygen atoms in their ground state.

3.4 $B^3\Sigma$

The electron impact excitation cross section of the $B^3\Sigma$ state from the ground state of O_2 has been measured by Wakiya[44] and calculated by Lin and Chung.[45] The experimental and theoretical cross sections are shown in Fig. 26. For electron energy below 20, where no experimental data is available, the shape of the theoretical cross section is used as a guide. At higher energies the cross section can be scaled with an E^{-1} dependence.

The excitation cross section for the $B^3\Sigma$ state is to be utilized as a dissociation cross section resulting in 0 and $O(^1D)$.

3.5 The Ionization and Dissociative Ionization of O_2

The total electron impact ionization cross section of O_2 has been measured by Tate and Smith[30] and Rapp and Englander-Golden,[29] for electron energies up to 1000 eV. Hirsh, et al.[34], have measured the ioni-

zation cross section at an electron energy of 1.5 MeV. The ionization cross section[29] is shown in Figure 27 and its extension to energies higher than 1000 eV can be made following the scaling law of $\sigma \sim E^{-1} \log CE$.

The dissociative ionization cross section is shown in Fig. 27 based on the measurement of Rapp, et al.[31]

The partial ionization cross sections leading to various ionization continua of O_2 are also given in Figure 27. These cross sections are based on data at 100 eV for the $b^4\Sigma$ state measured by McConkey and Woolsey.[46] The measurements of Skubenich[47] for the cross sections of $b^4\Sigma$ and $A^2\pi$ states are utilized for the relative ratio between these two states. This ratio is used to obtain the cross section for the $A^2\pi$ state, by utilizing McConkey and Woolsey data for $b^4\Sigma$ state. Subtracting the cross section values of $b^4\Sigma$, $A^2\pi$ and the dissociative ionization from the total ionization cross section one obtains the sum for the excitation of the $X^2\pi$ and $a^4\pi$ states. This sum then is divided between $X^2\pi$ and $a^4\pi$ states according to their statistical weights.

4. Oxygen Atom

4.1 Oxygen Atom Low Lying Metastable States $O(^1D)$ and $O(^1S)$

The electron impact excitation cross sections for the low lying metastable states of oxygen atom have been calculated by numerous investigators.[48-50] There seems to be good agreement between these calculations, especially for the excitations of ^1S state. For the excitation of $O(^1D)$, however, the difference in the slope of the cross sections at threshold and near threshold is apparent. The calculated cross section by Thomas and Nisbet[49] is preferred. No experimental data are available on these cross sections.

4.2 Optically Allowed Transitions

For optically allowed transitions, the following expression,

given by Drawin,[51] will be utilized.

$$\sigma = 3.5 \times 10^{-16} f_{ij} \left(\frac{13.6}{E_{ij}}\right)^2 \left(\frac{E_{ij}}{E}\right)^2 \left(\frac{E}{E_{ij}} - 1\right) \log \left(1.25 \frac{E}{E_{ij}}\right)$$

Here, f_{ij} is the oscillator strength for the transition i → j whose excitation energy is E_{ij} and E is the electron energy. Using this expression, the electron impact excitation cross sections for few optically allowed transitions are given in Figure 29. The above expression used for the transition $^3P - {}^3S$ (the resonance line) yield a peak value which is lower by a factor of ∿ 2 compared to a measurement by Stone and Zopf[52].

4.3 Ionization Cross Section of O

The electron impact ionization cross section of oxygen atom has been measured by Fite and Brackmann[53] and is shown in Figure 30. The decomposition of the total ionization cross section into various ionization continua of O^+, i.e. $O^+(^4S)$, $O^+(^2D)$ and $O^+(^2P)$ can be made using Table 1. The percentage of the fractional ionization cross sections are given as a function of the electron energy. Data for Table 1 for electron energy up to 100 eV is from Dalgarno and Lejeune.[54]

Table 1

Partial Ionization Cross Section of Oxygen Atom

Electron Energy (eV)	$O^+(^4S)$	$O^+(^2D)$	$O^+(^2P)$
25	0.5	0.36	0.13
50	0.39	0.41	0.20
75	0.37	0.42	0.21
100	0.36	0.42	0.22
E>100	0.36	0.42	0.22

5. Nitrogen Atom

5.1 Low lying Metastable States $N(^2D)$ and $N(^2P)$

The electron impact excitation cross sections for the low lying metastable states, $N(^2D)$ and $N(^2P)$, have been calculated by several investigators.[48,55,56] These calculated cross sections are shown in Figures 31-33. The calculations of Berrington, et al.[55] is to be preferred because they include the effects of target polarization, higher lying configurations and short range correlations.

5.2 Optically Allowed Transitions

For optically allowed transitions one can utilize the cross section expression given in Section 4.2 of this report. Using this expression the excitation cross sections for two optically allowed states are illustrated in Figure 34. For the rest of the optically allowed states one generally needs the excitation energies and the oscillator strengths which can be found in Ref. 57.

5.3 Ionization Cross Section of Nitrogen Atoms

The electron impact ionization cross section of nitrogen atom has been measured[58] and is shown in Figure 35.

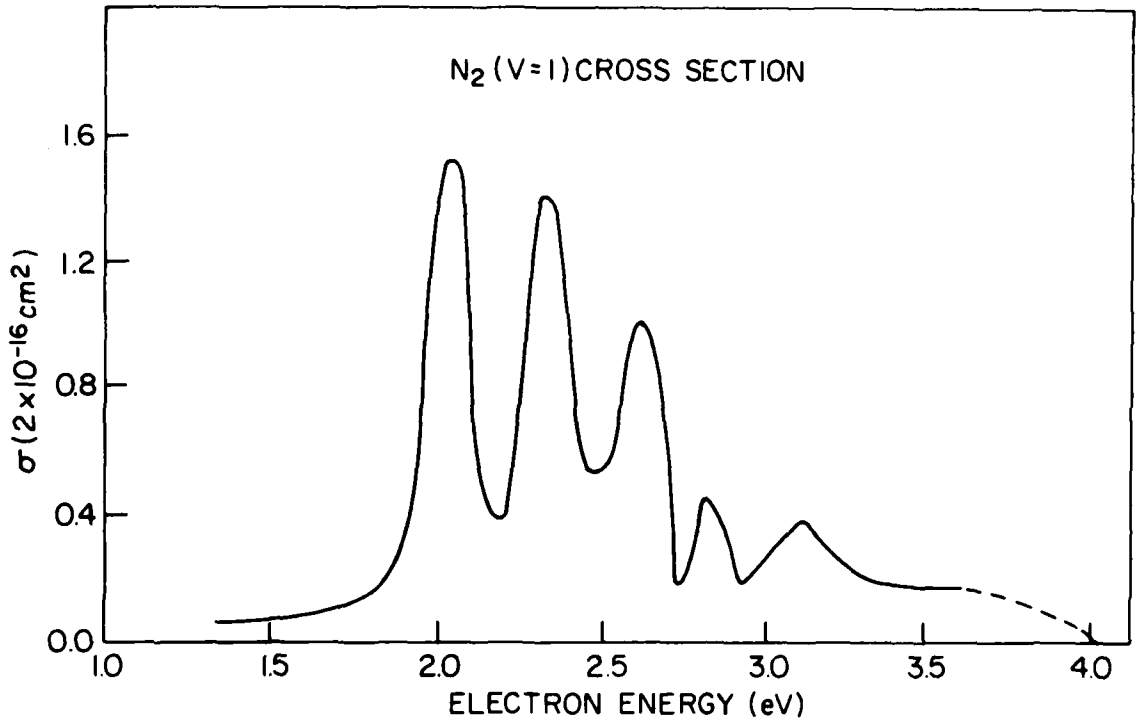

Fig. 1 — The cross section for the electron impact excitation of the first ground state vibrational level of N_2

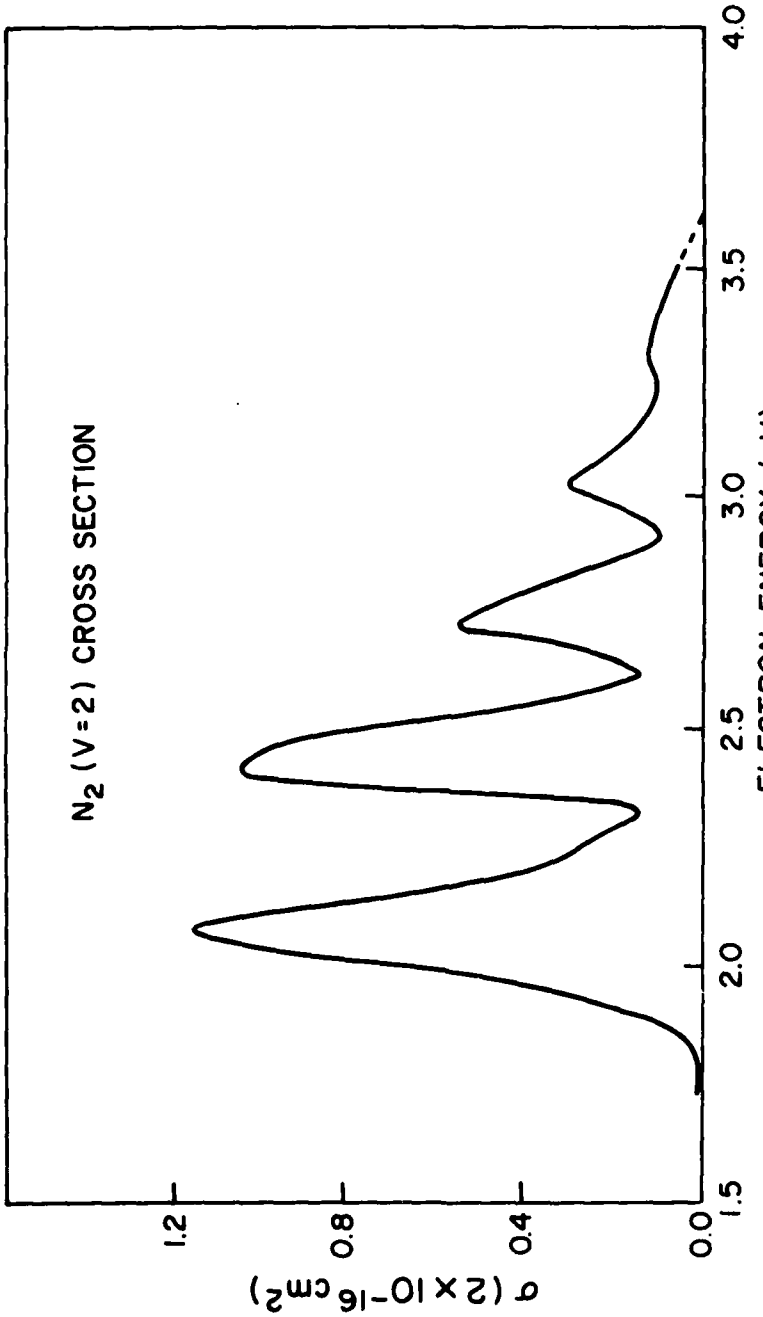

Fig. 2 — The cross section for the electron impact excitation of the second ground state vibrational level of N_2

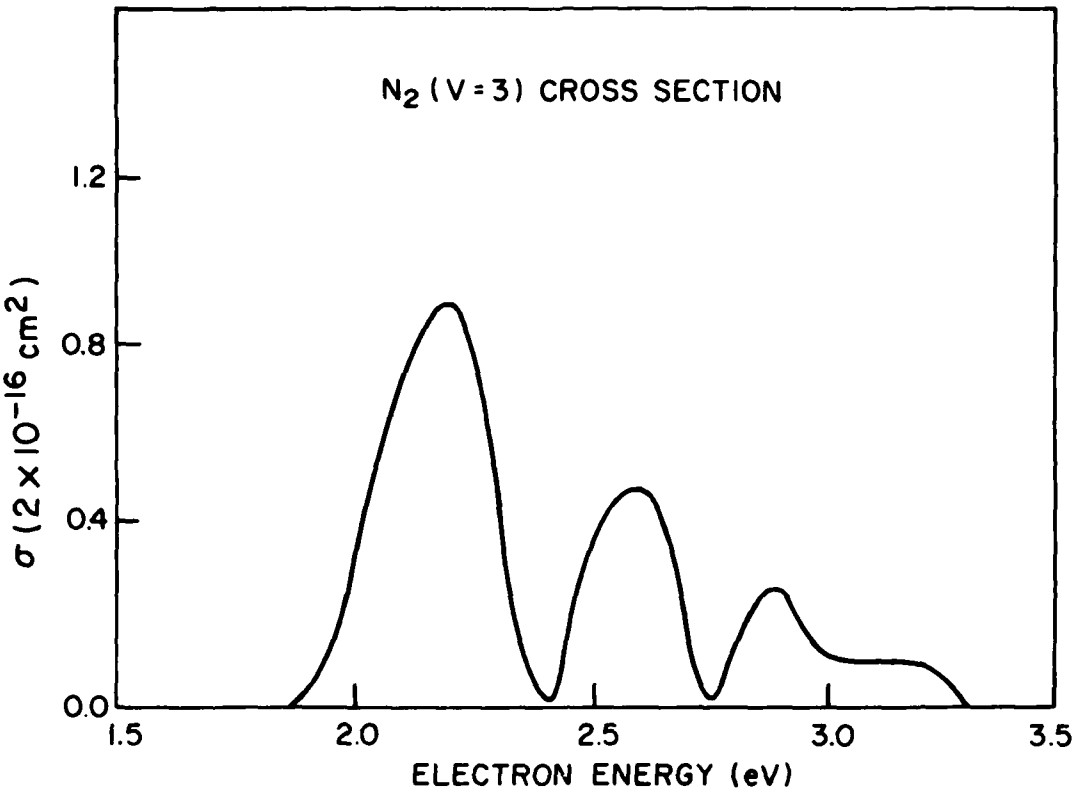

Fig. 3 — The cross section for the electron impact excitation of the third ground state vibrational level of N_2

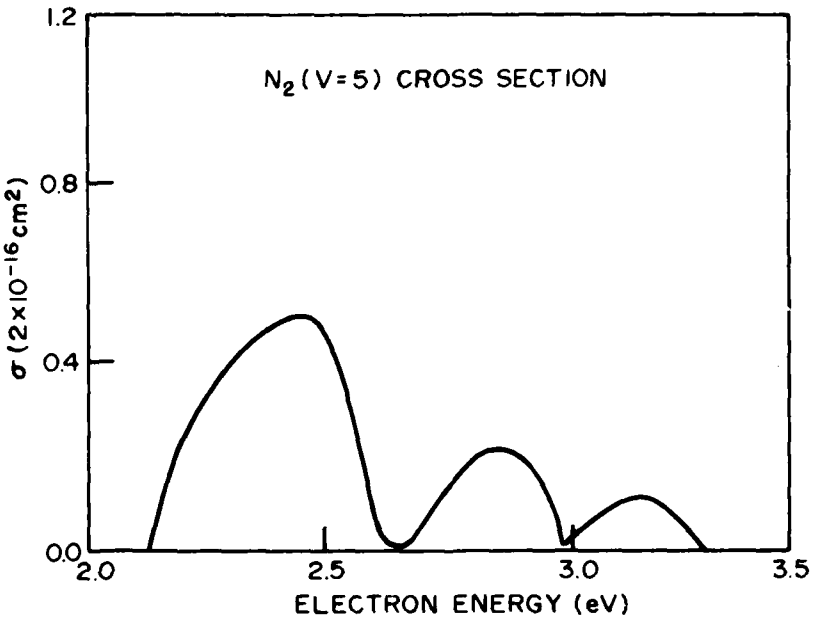

Fig. 4 — The cross section for the electron impact excitation of the fourth ground state vibrational level of N_2

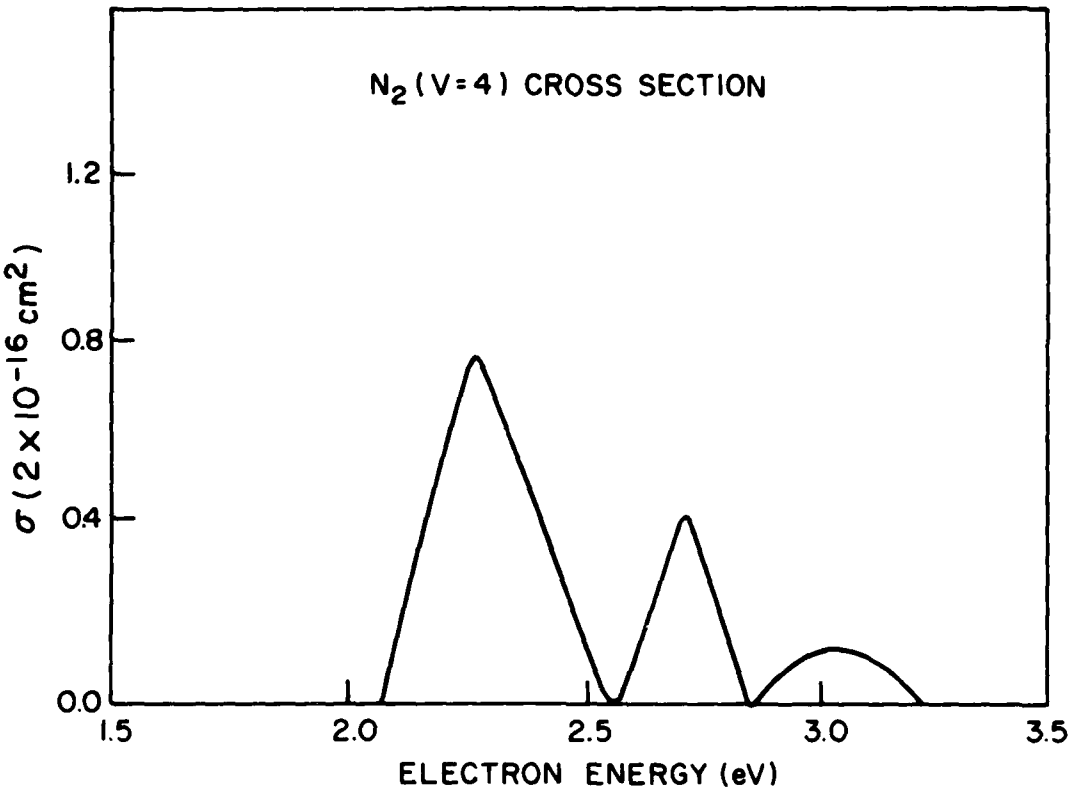

Fig. 5 — The cross section for the electron impact excitation of the fifth ground state vibrational level of N_2

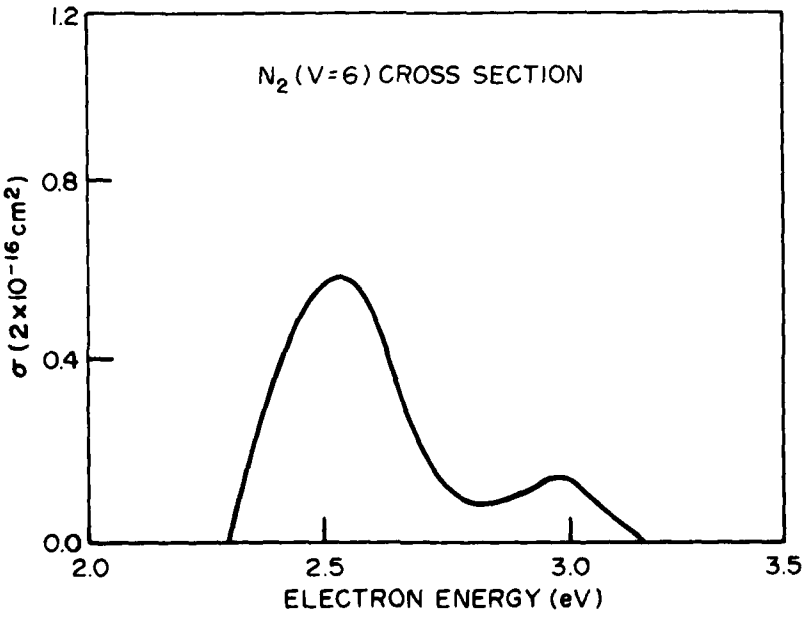

Fig. 6 — The cross sectional for the electron impact excitation of the sixth ground state vibrational level of N_2

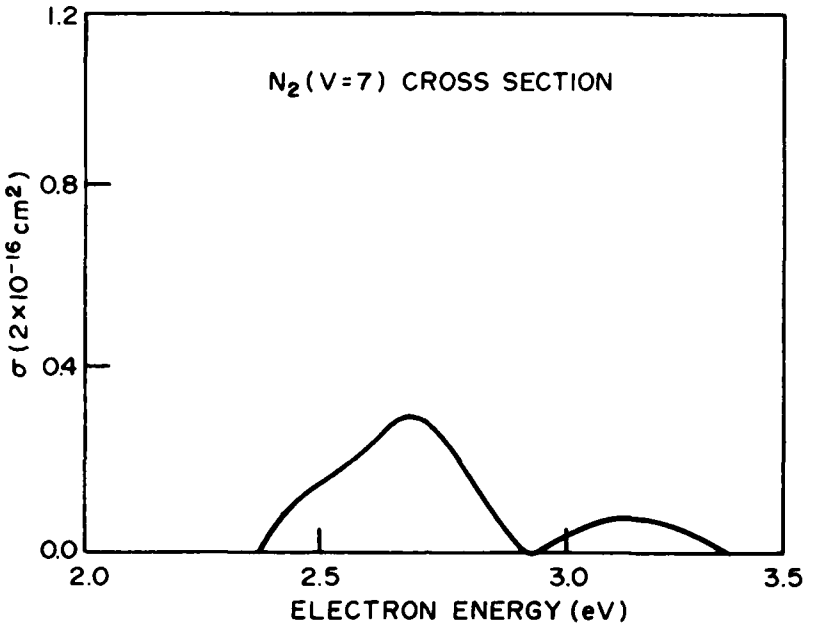

Fig. 7 — The cross section for the electron impact excitation of the seventh ground state vibrational level of N_2

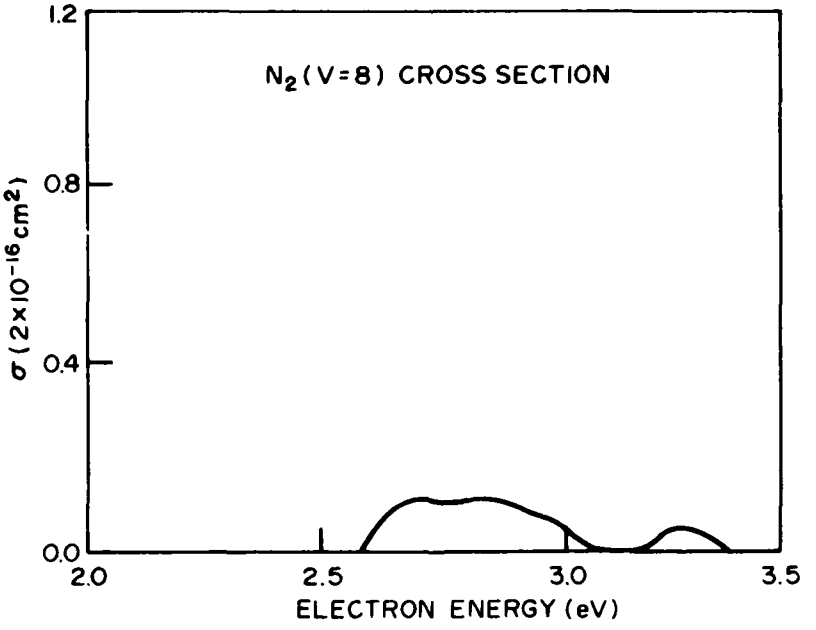

Fig. 8 — The cross section for the electron impact excitation of the eighth ground state vibrational level of N_2

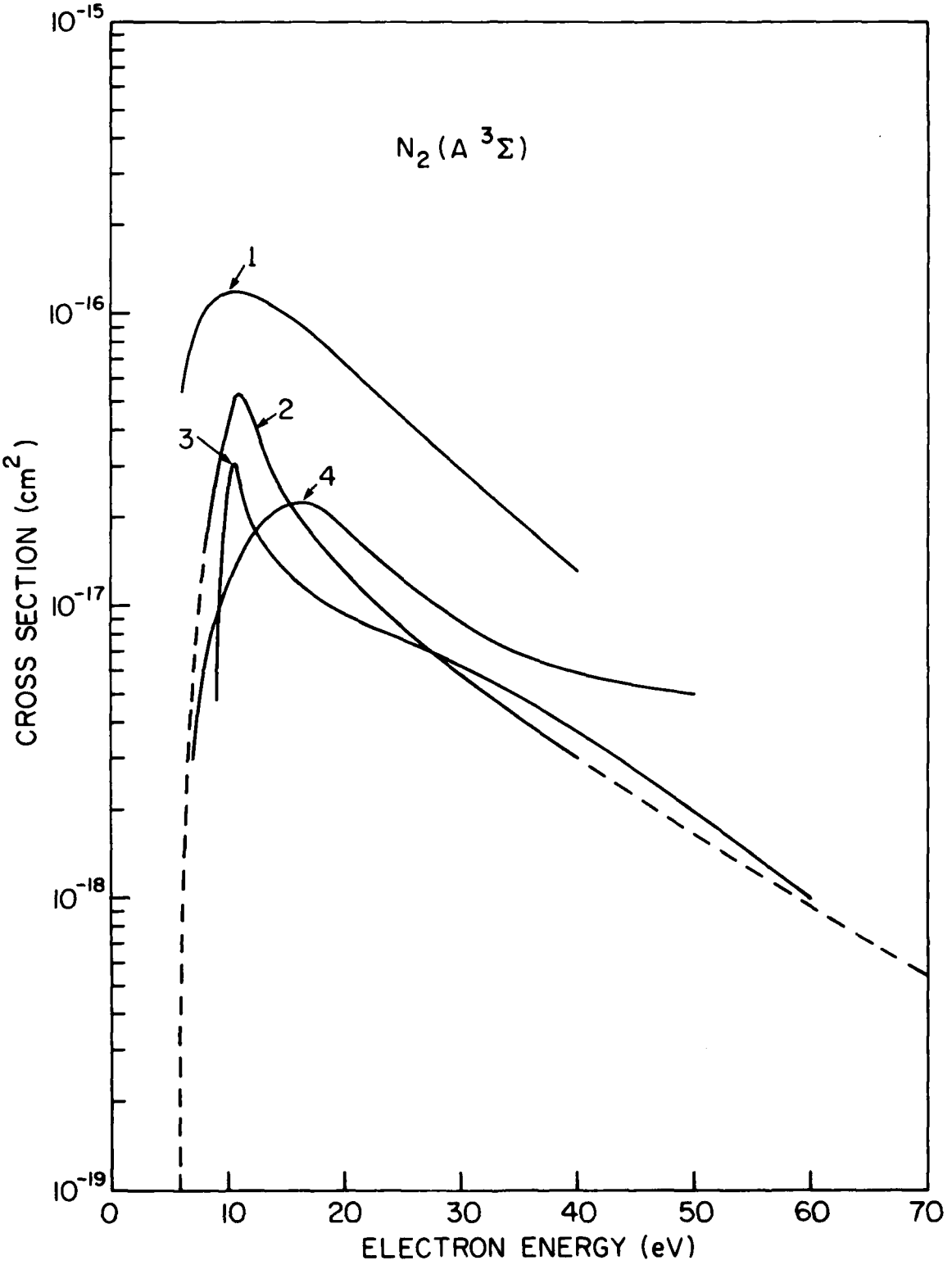

Fig. 9 — The cross section for the electron impact excitation of $N_2(A^3\Sigma)$. Curves designated 1, 2, 3 and 4 refer to data from references (10), (12), (11) and (13), respectively.

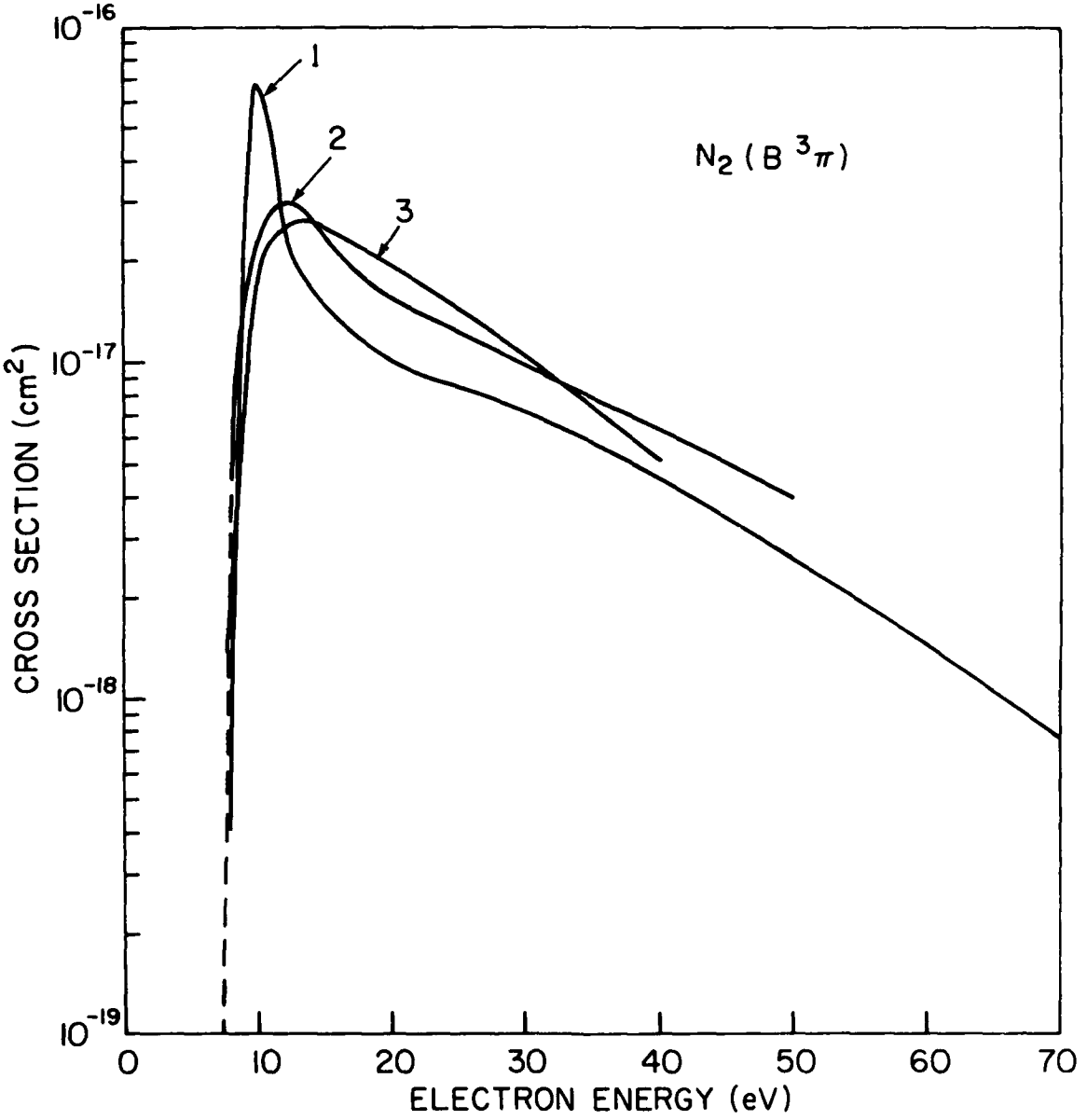

Fig. 10 — The cross section for the electron impact excitation of $N_2(B^3\pi)$. Curves designated 1, 2 and 3 refer to data from references 11, 13 and 10 respectively.

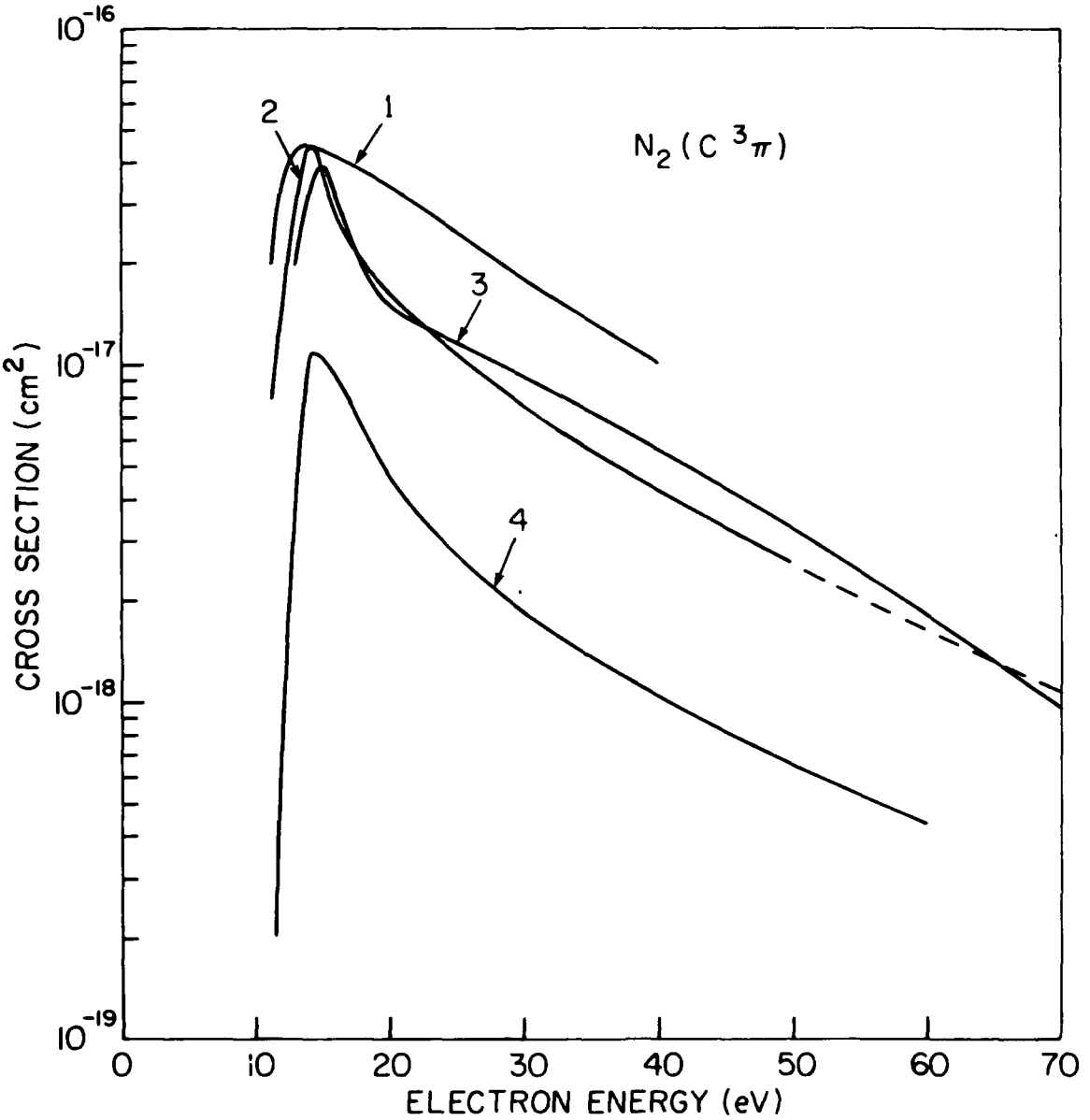

Fig. 11 — The cross section for the electron impact excitation of $N_2(C^3\pi)$. Curves designated 1, 2 and 3 refer to data from references 10, 13 and 11, respectively. The curve designated 4 is from reference (16) and is the cross section for the (o,o) band emission at 3371 Å.

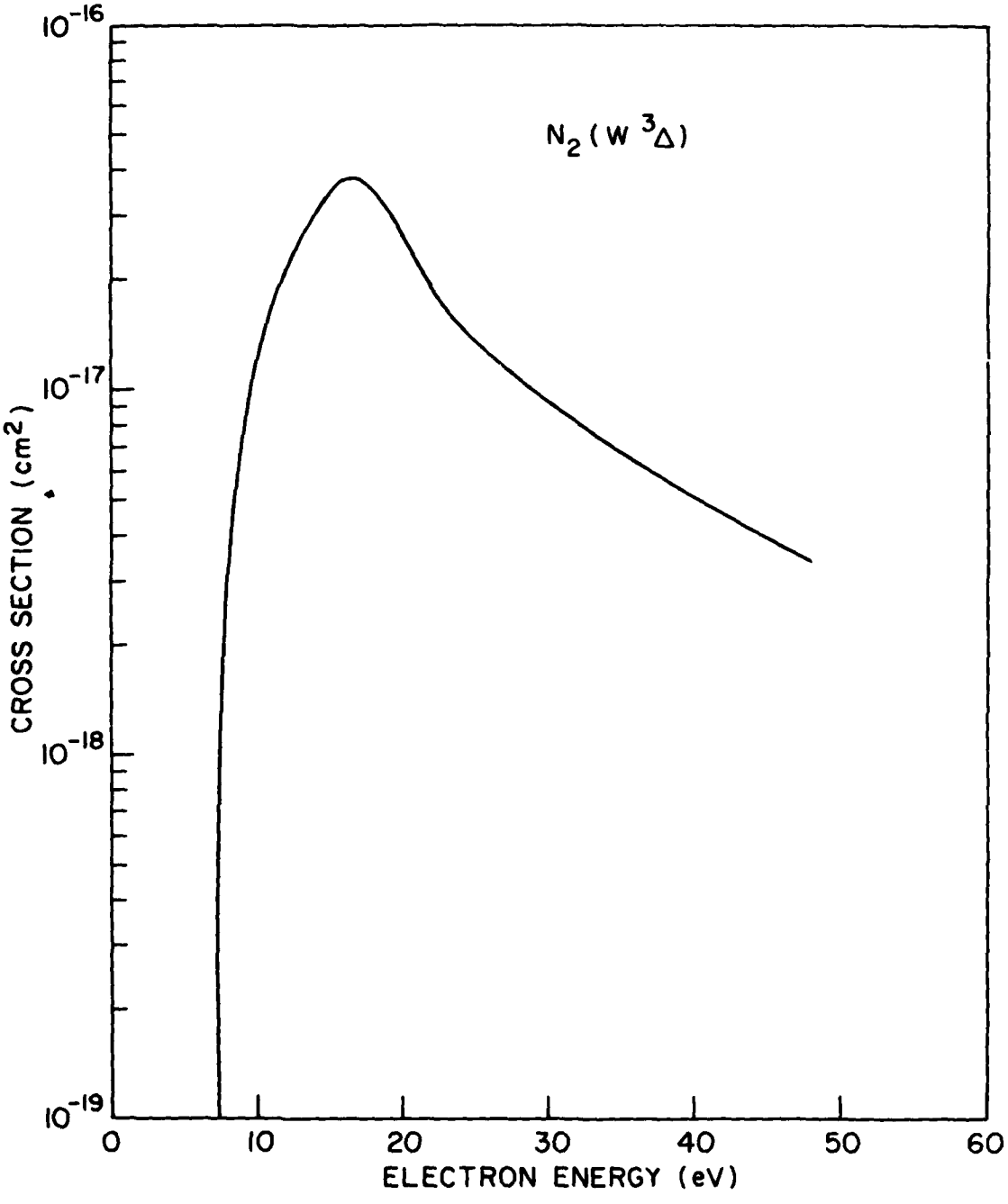

Fig. 12 — The cross section for the electron impact excitation of $N_2(W^3\Delta)$. Data is from reference 13.

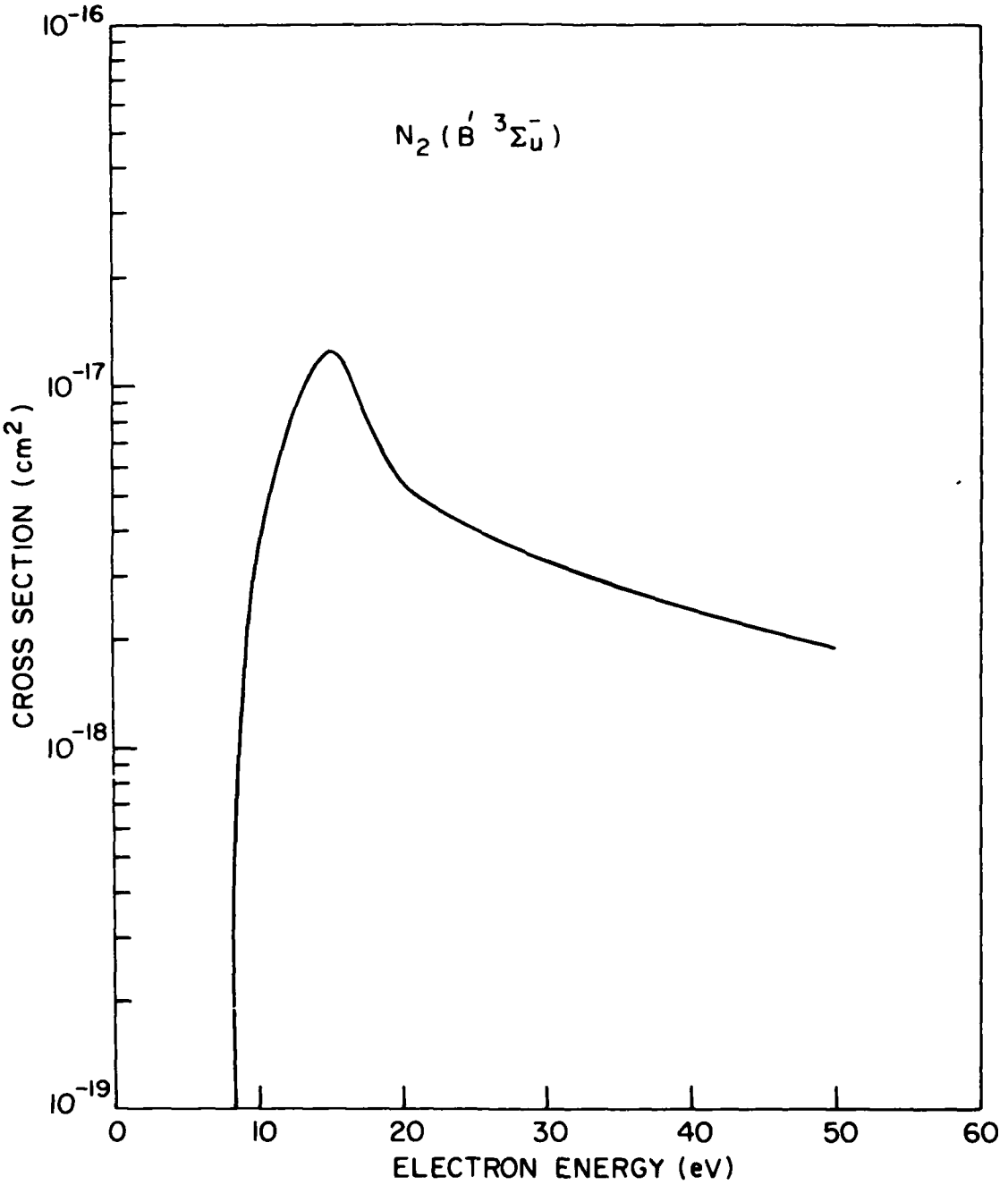

Fig. 13 — The cross section for the electron impact excitation of $N_2(B'\ ^3\Sigma)$. Data is from reference 13.

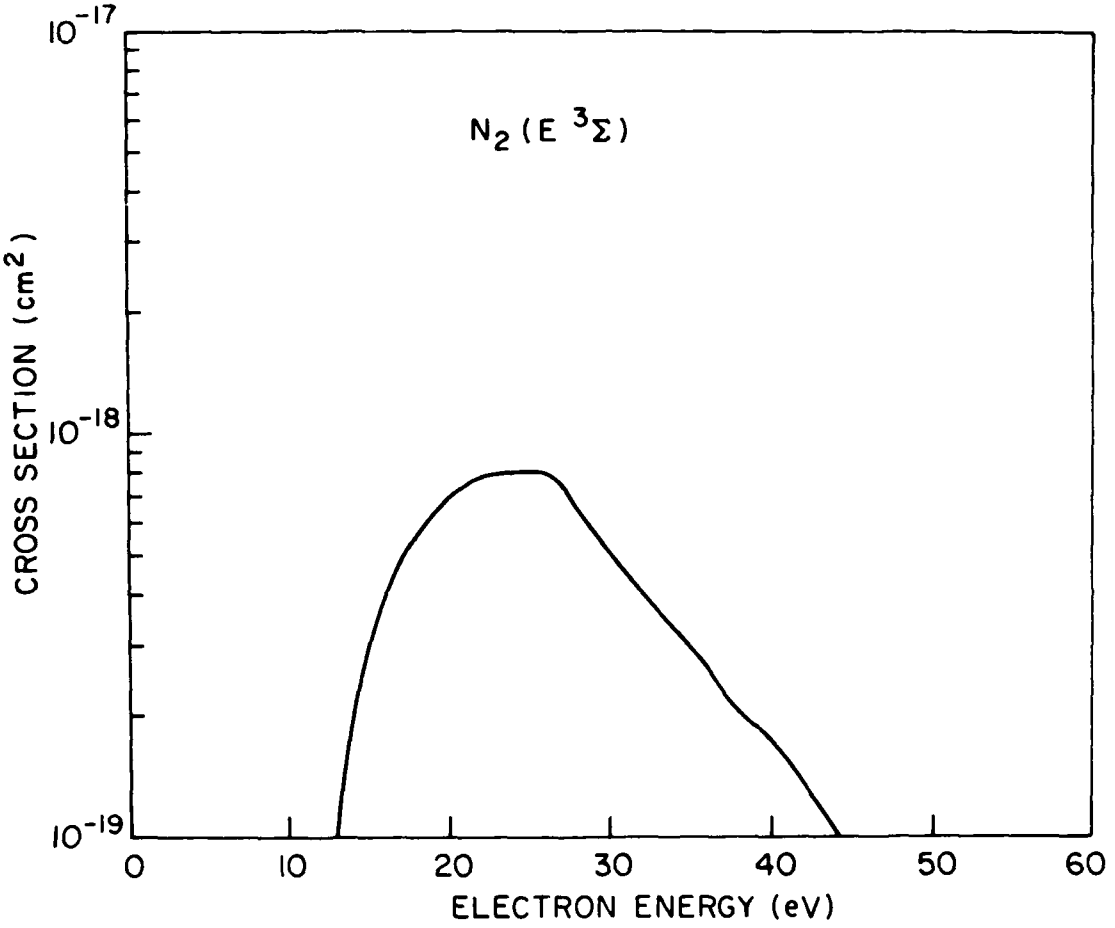

Fig. 14 — The cross section for the electron impact excitation of $N_2(E^3\Sigma)$. Data is from reference 13.

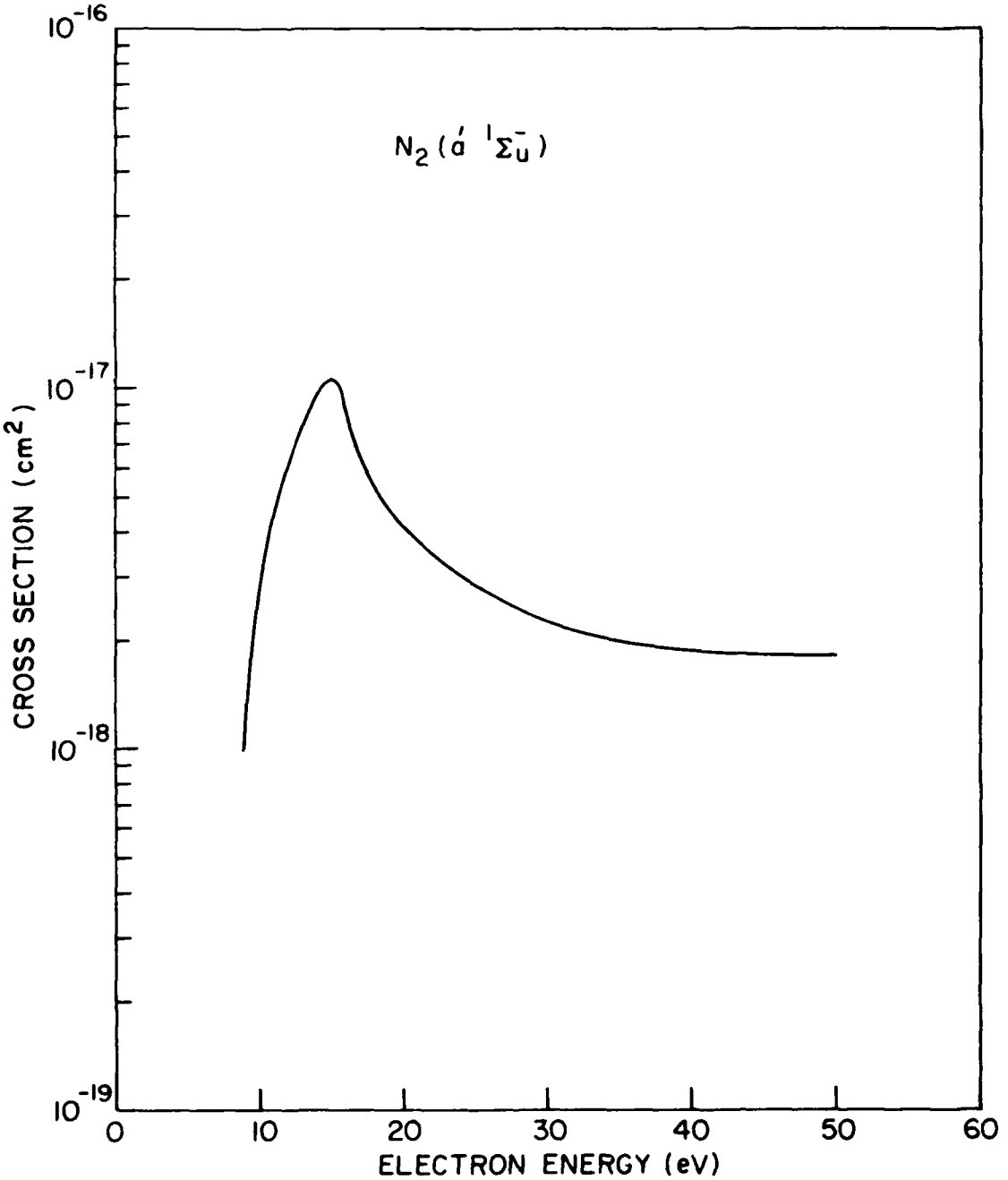

Fig. 15 — The cross section for the electron impact excitation of $N_2(a'\ ^1\Sigma_u)$

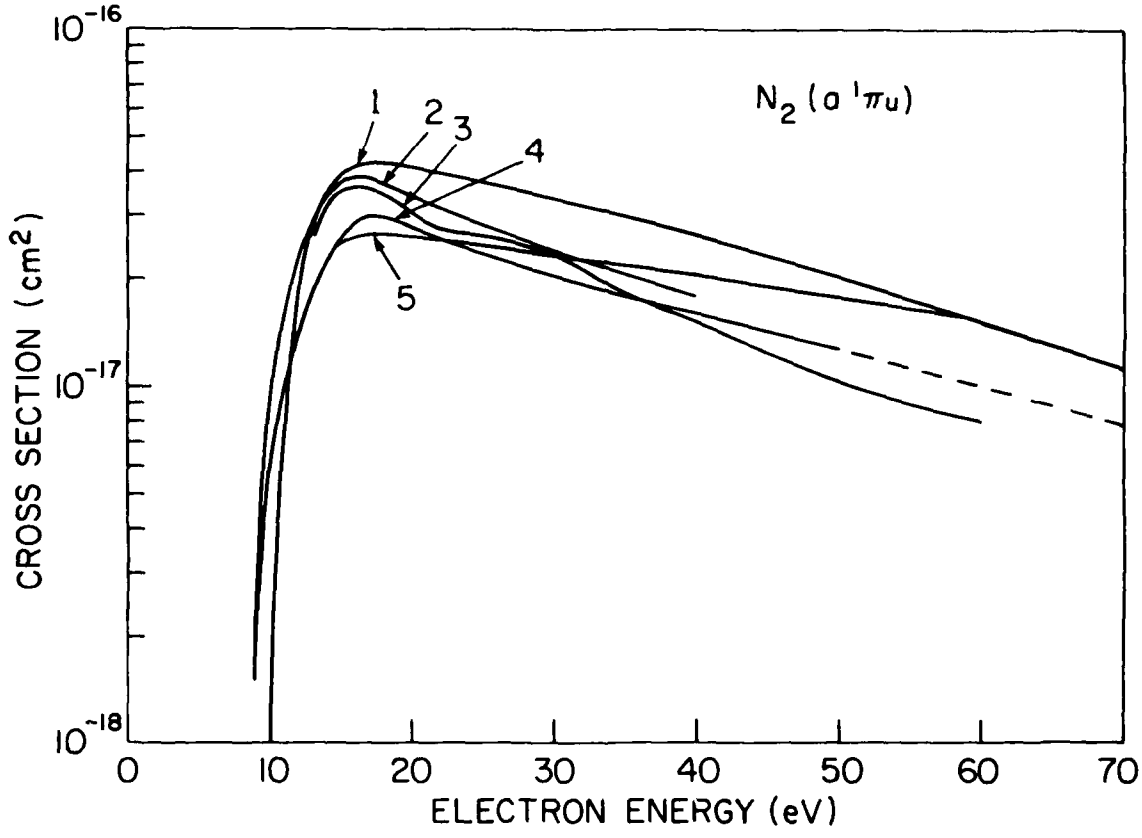

Fig. 16 — The cross section for the electron impact excitation of $N_2(a\ ^1\pi_u)$. Curves 1, 2, 3, 4 and 5 designate data from references 11, 12, 19, 13 and 10, respectively.

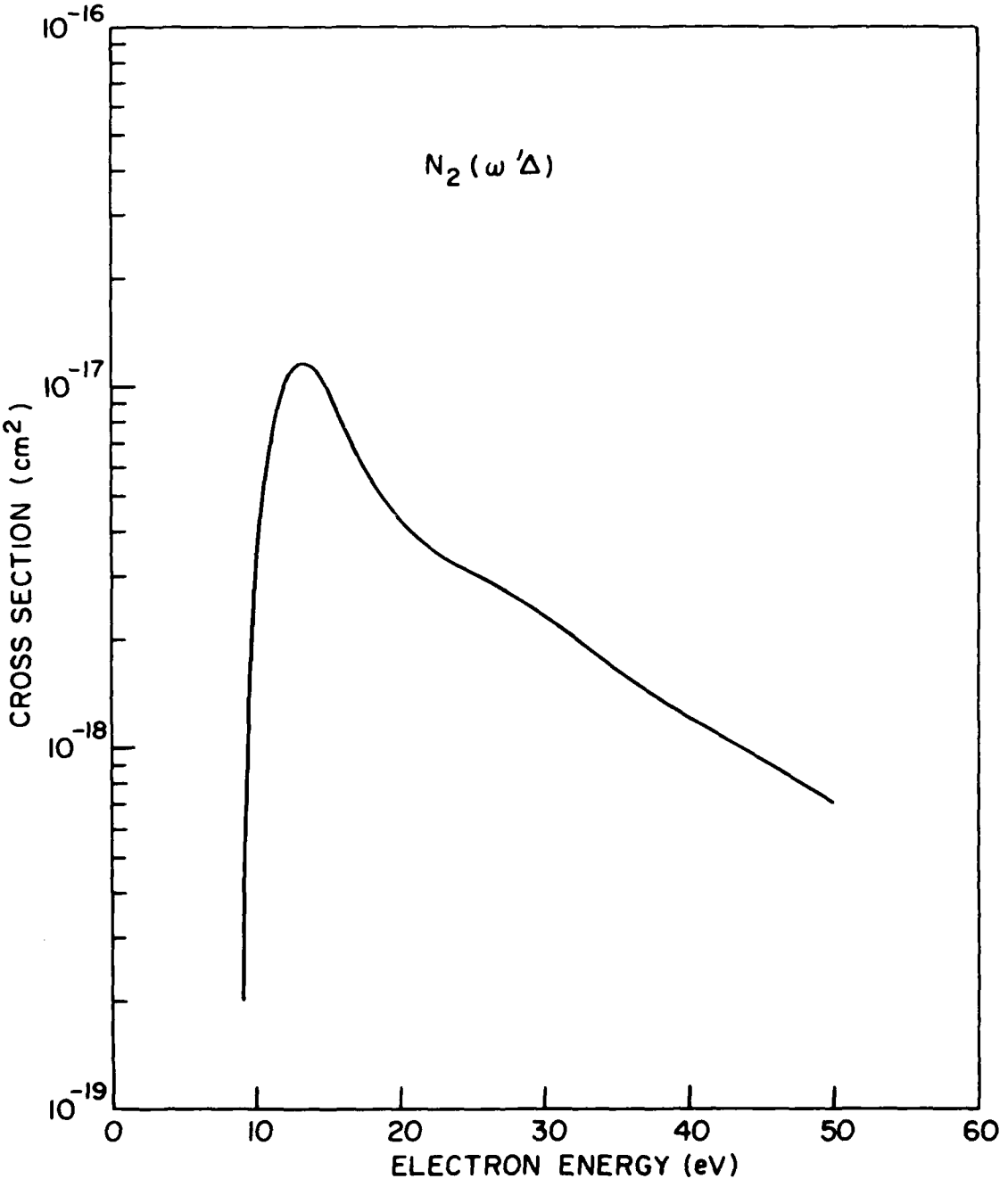

Fig. 17 — The cross section for the electron impact excitation of $N^2(W^1\Delta)$. Data is from reference 13.

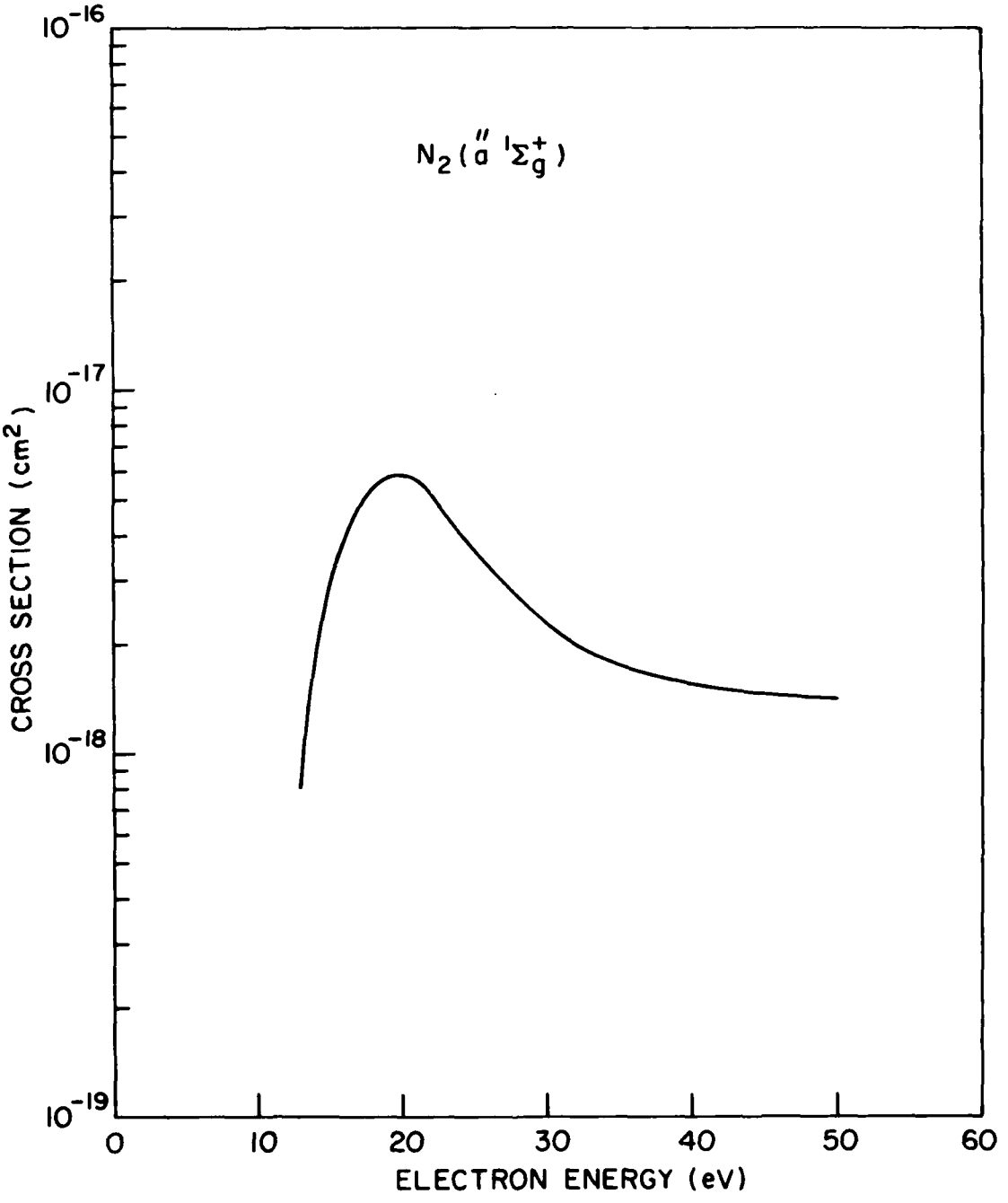

Fig. 18 — The cross section for the electron impact excitation of $N_2(a'' {}^1\Sigma g)$. Data is from reference 13.

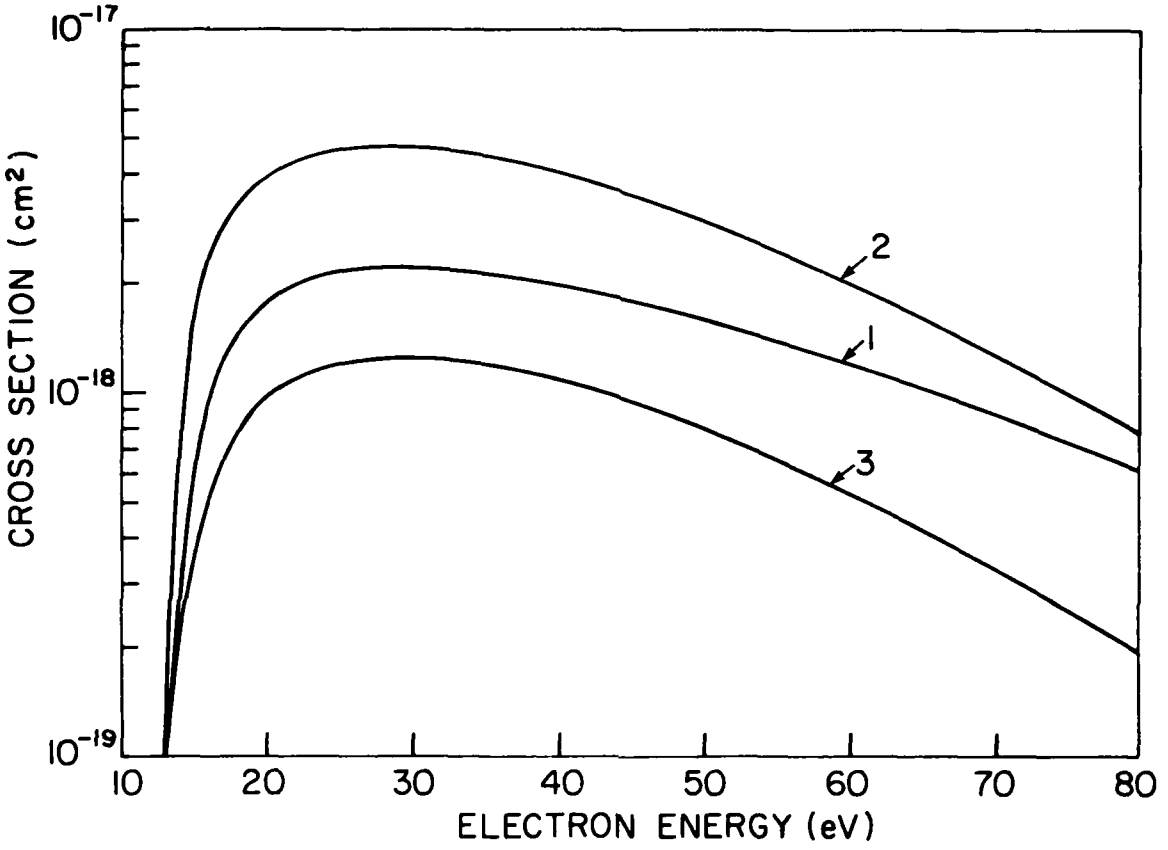

Fig. 19 — The cross section for the electron impact excitation of $N_2(F^3\Pi_u)$. $N_2(G^3\Pi_u)$ and M_1 states indicated as 1, 2 and 3, respectively. Data are from reference 21.

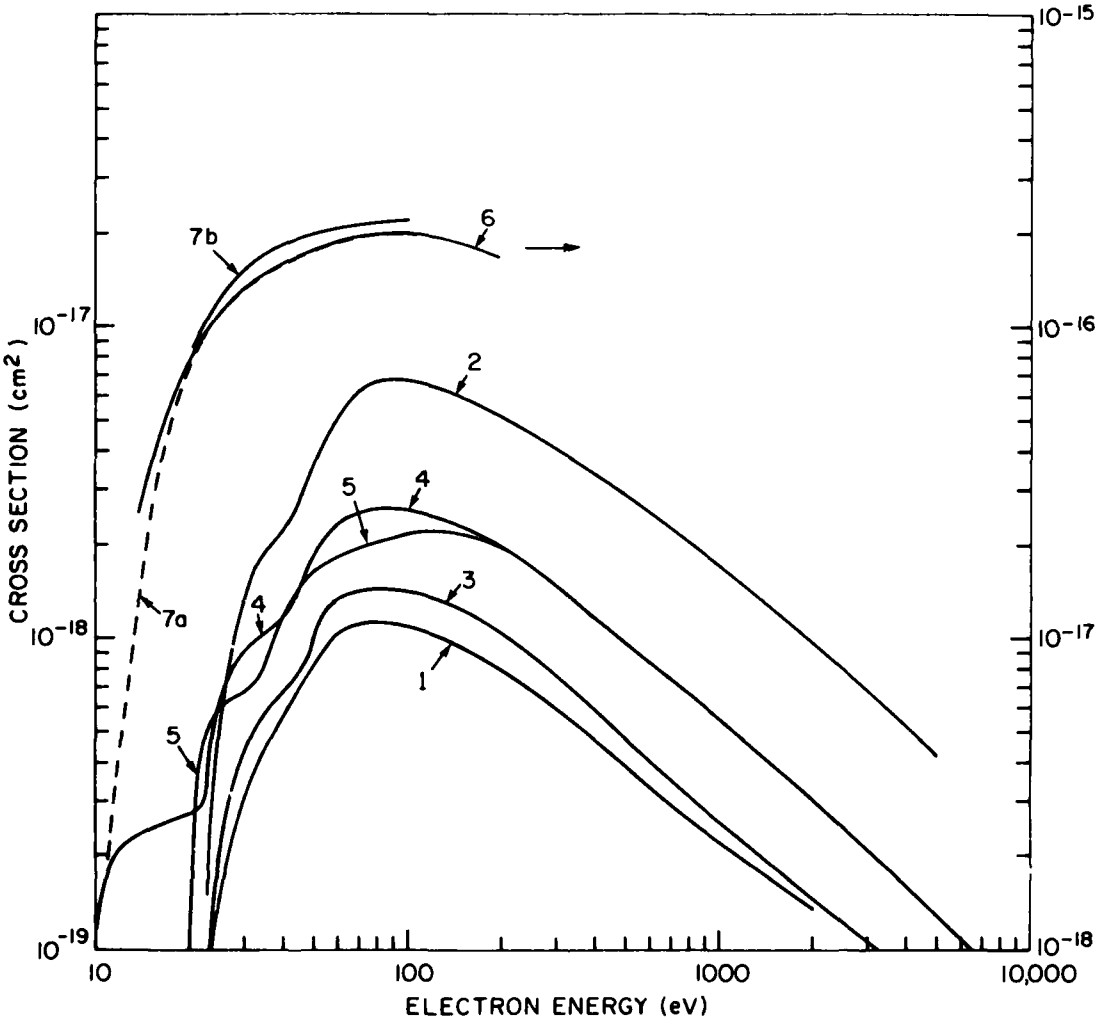

Fig. 20 — Cross sections for the electron impact dissociative excitation emission at 1134 Å, 1200 Å, 1243 Å, 1493 Å and 1743 Å shown as curves 1, 2, 3, 4 and 5, respectively. (See text for references.) The N_2 dissociation cross section is shown as curves 6 (ref. 22) and 7a and 7b (ref. 23), where a and b indicate optically thick and thin cases.

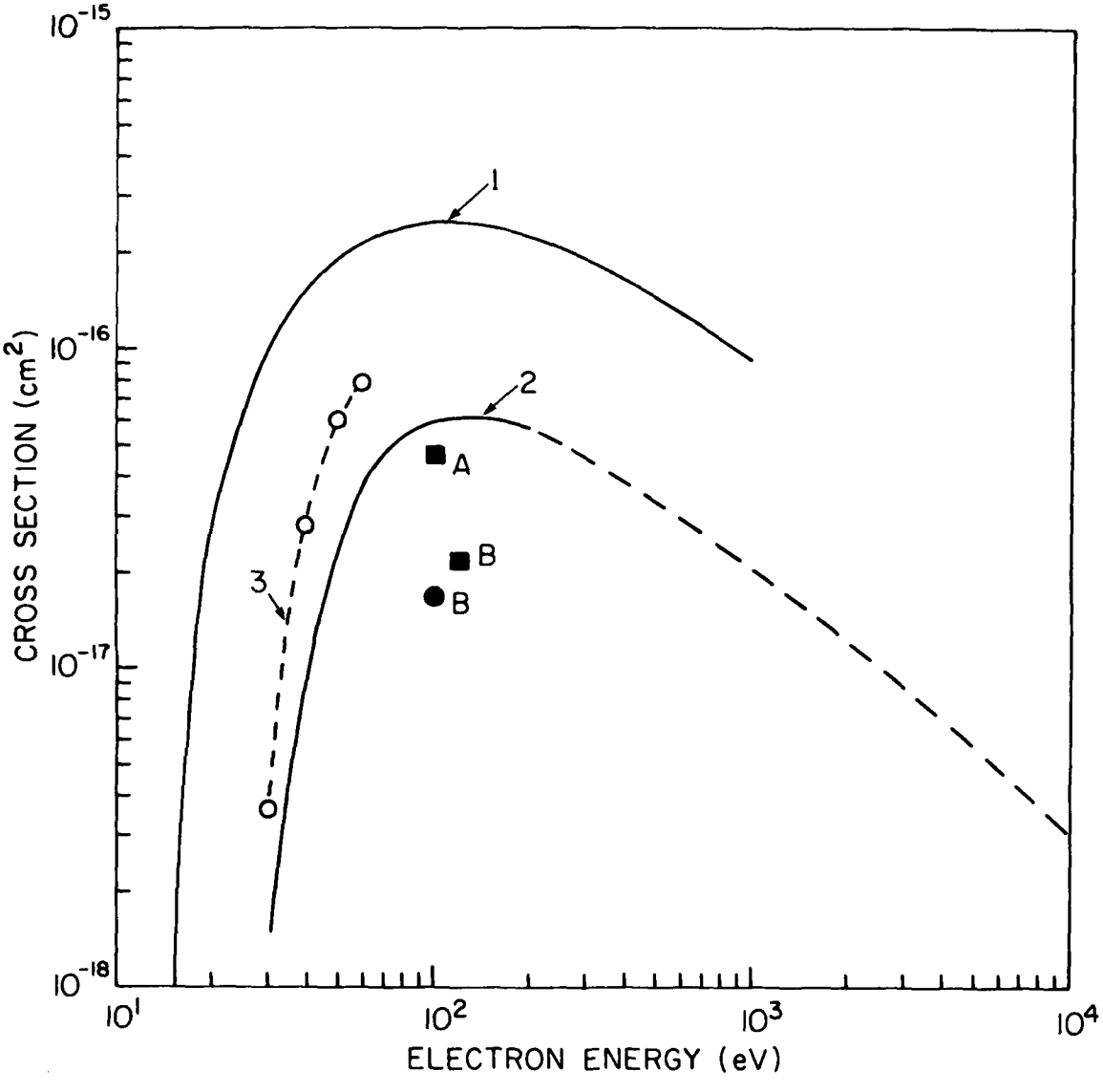

Fig. 21 — The N_2 ionization cross section is shown as curve 1 (ref. 29). The N_2 dissociative ionization is shown as curves 2 (ref. 31) and 3 (ref. 32). The peak cross sections for ionization leading to $N_2^+(A)$, $N_2^+(B)$ and for emission at 3914 Å are indicated □A, □B and ○B, respectively.

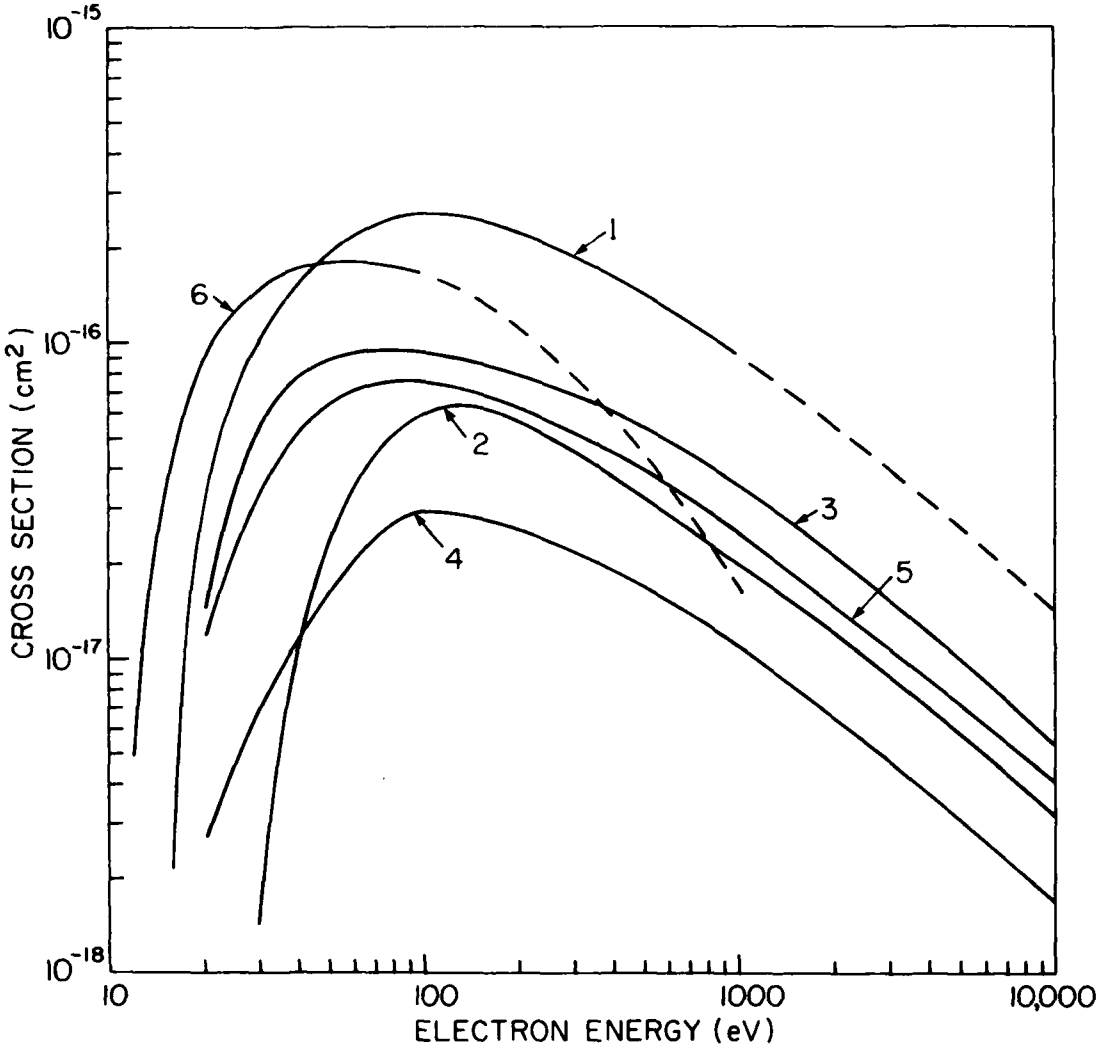

Fig. 22 — The electron impact ionization and dissociative ionization of N_2 are designated as curves 1 and 2, respectively. Curves 3, 4 and 5 are the partial ionization cross sections leading to $N_2^+(X)$, $N_2^+(A)$ and $N_2^+(B)$ states. Curve 6 indicates the pure dissociative cross section of N_2.

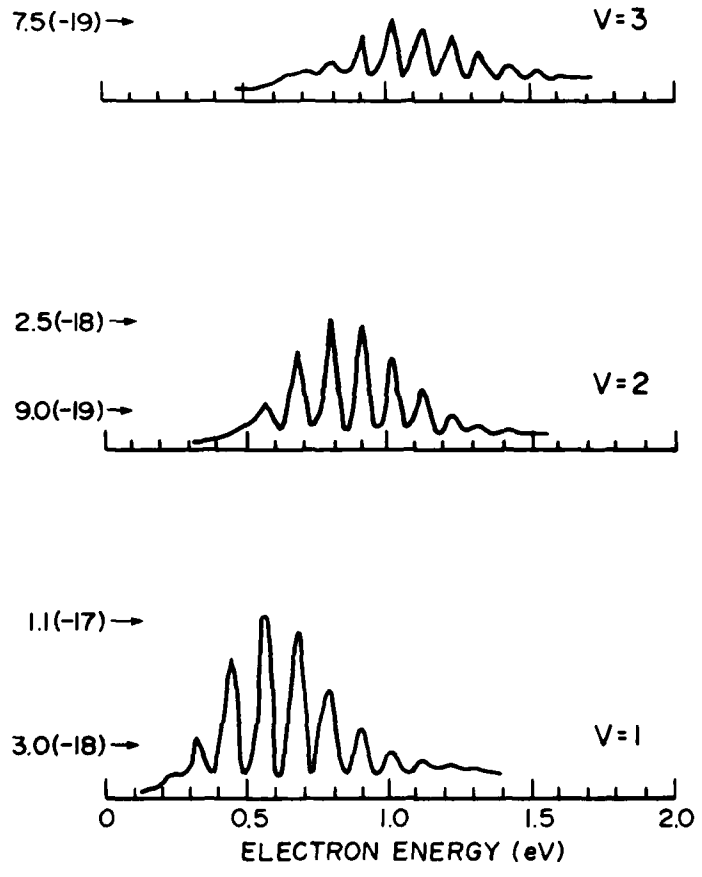

Fig. 23 — The electron impact excitation cross section for the ground state vibrational level of O_2 (ref. 38)

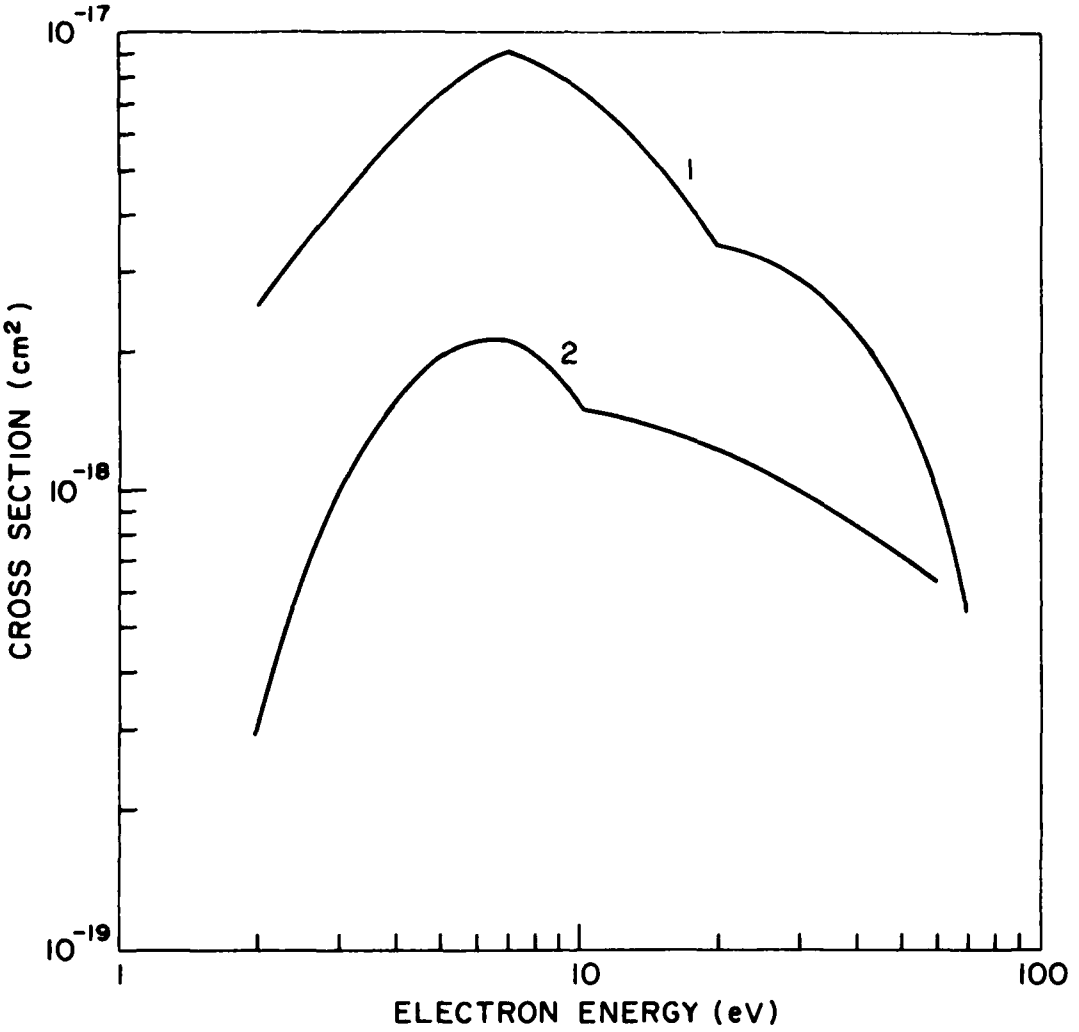

Fig. 24 — The electron impact excitation cross section of $O_2(a^1\Delta)$ and $b^1\Sigma$. (See text for references.)

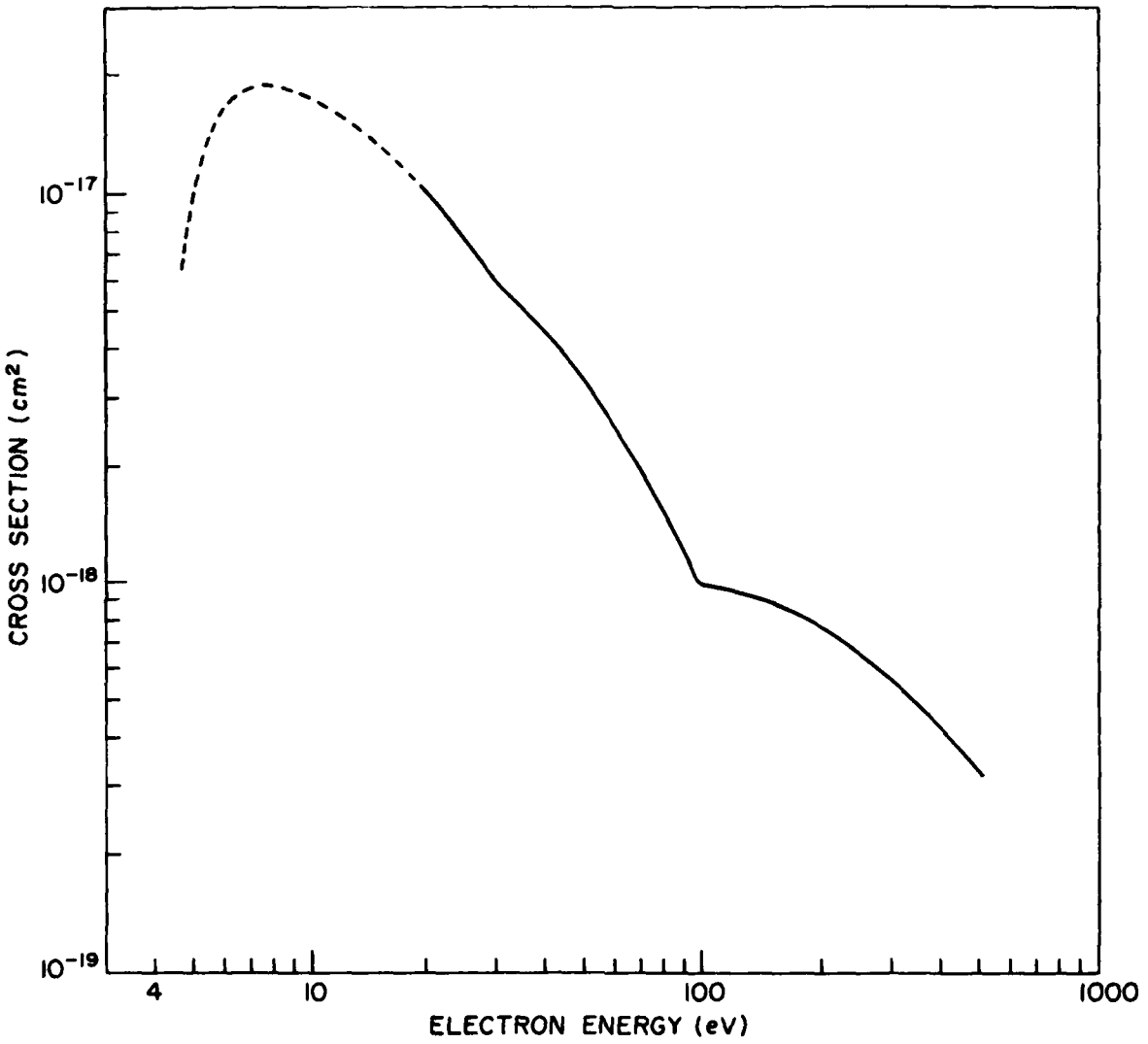

Fig. 25 — The electron impact excitation cross section for O_2 states of $A^3\Sigma + C^3\Delta + C^1\Sigma$

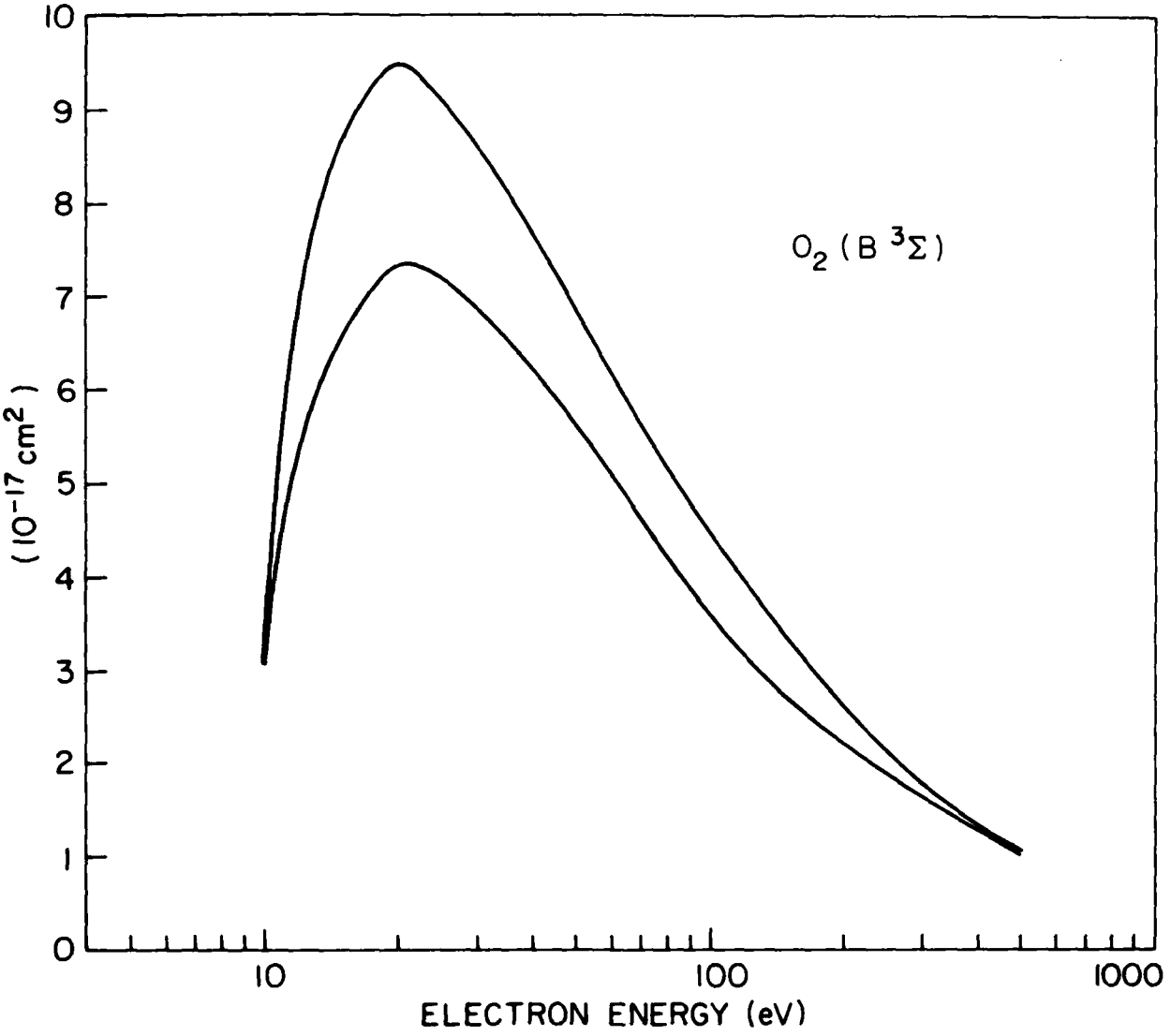

Fig. 26 — Cross section for the electron impact excitation of $O_2(B^3\Sigma)$. Curve 1 (ref. 15), curve 2 (ref. 44). Also see text.

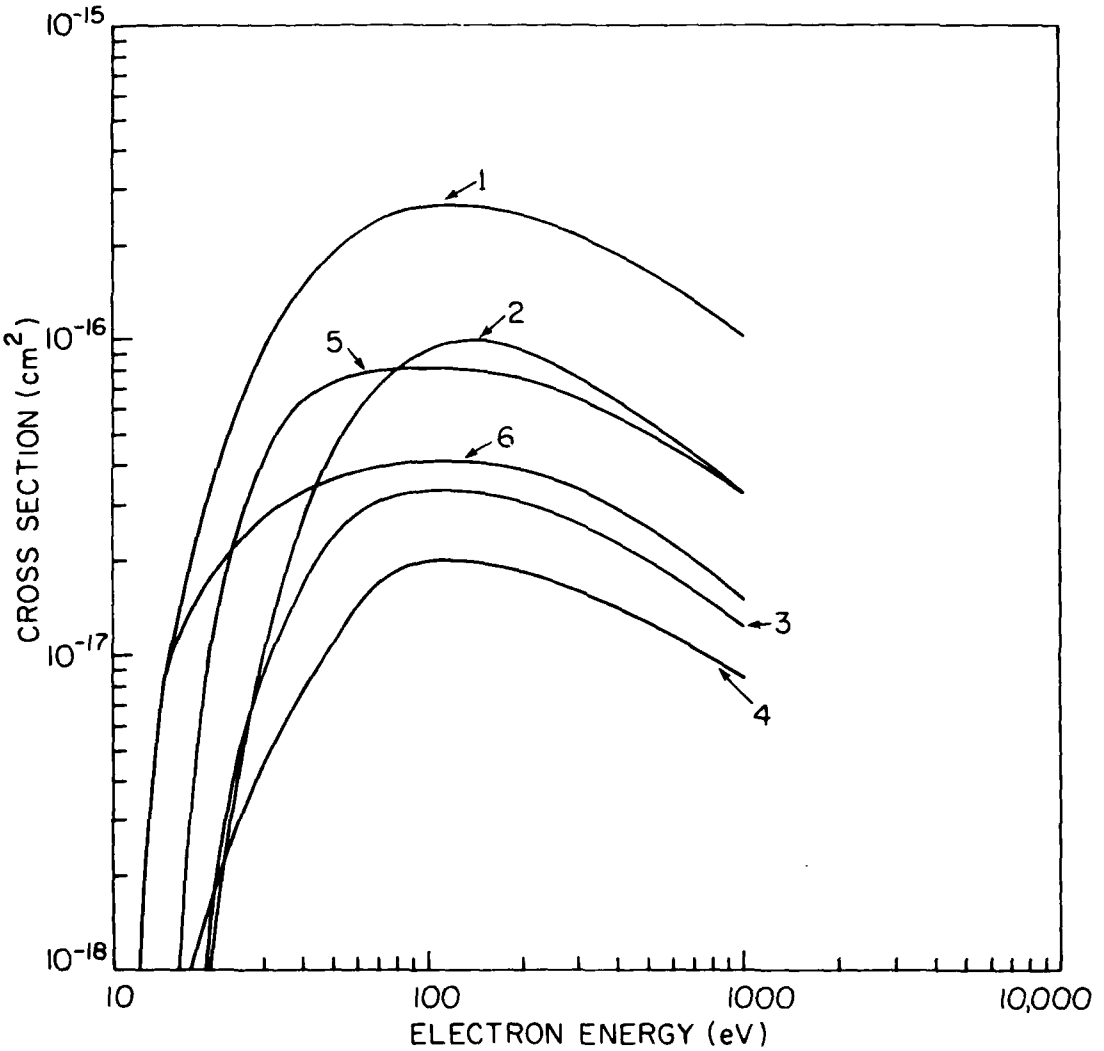

Fig. 27 — Cross section for the electron impact ionization and dissociative ionization of O_2 indicated as curves 1 (ref. 29) and 2 (ref. 31), respectively. The partial ionization cross section leading to $b^4\pi$, $A^2\pi$, $a^4\pi$ and $x^2\pi$ states are designated as curves 3, 4, 5 and 6, respectively. (See text for detail.)

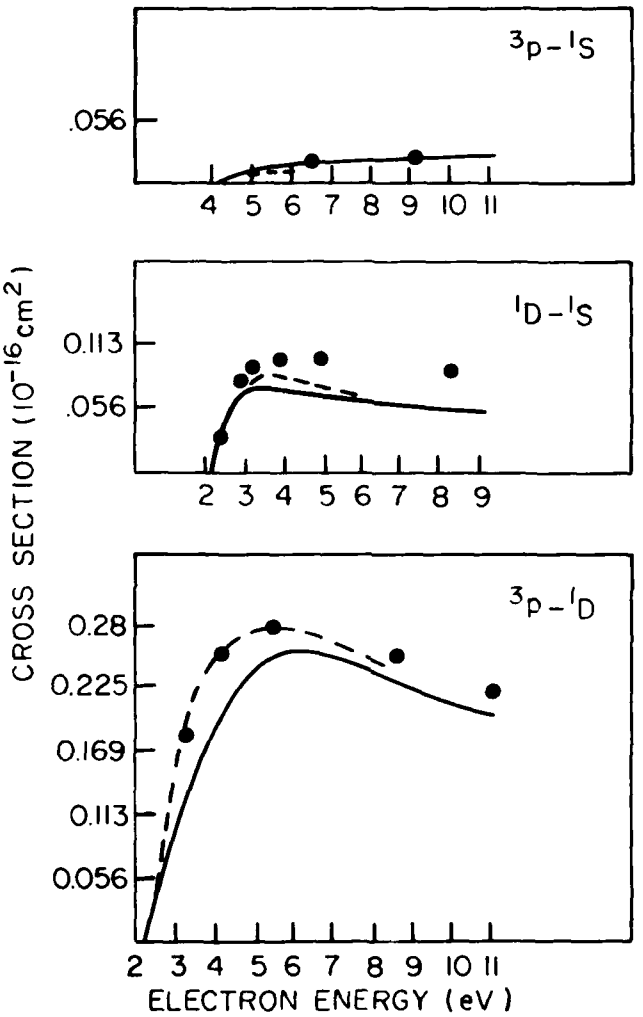

Fig. 28 — Electron impact excitation cross sections for low lying metastable states of oxygen atom, solid curve (ref. 49), dashed curve (ref. 50) and circles (ref. 48)

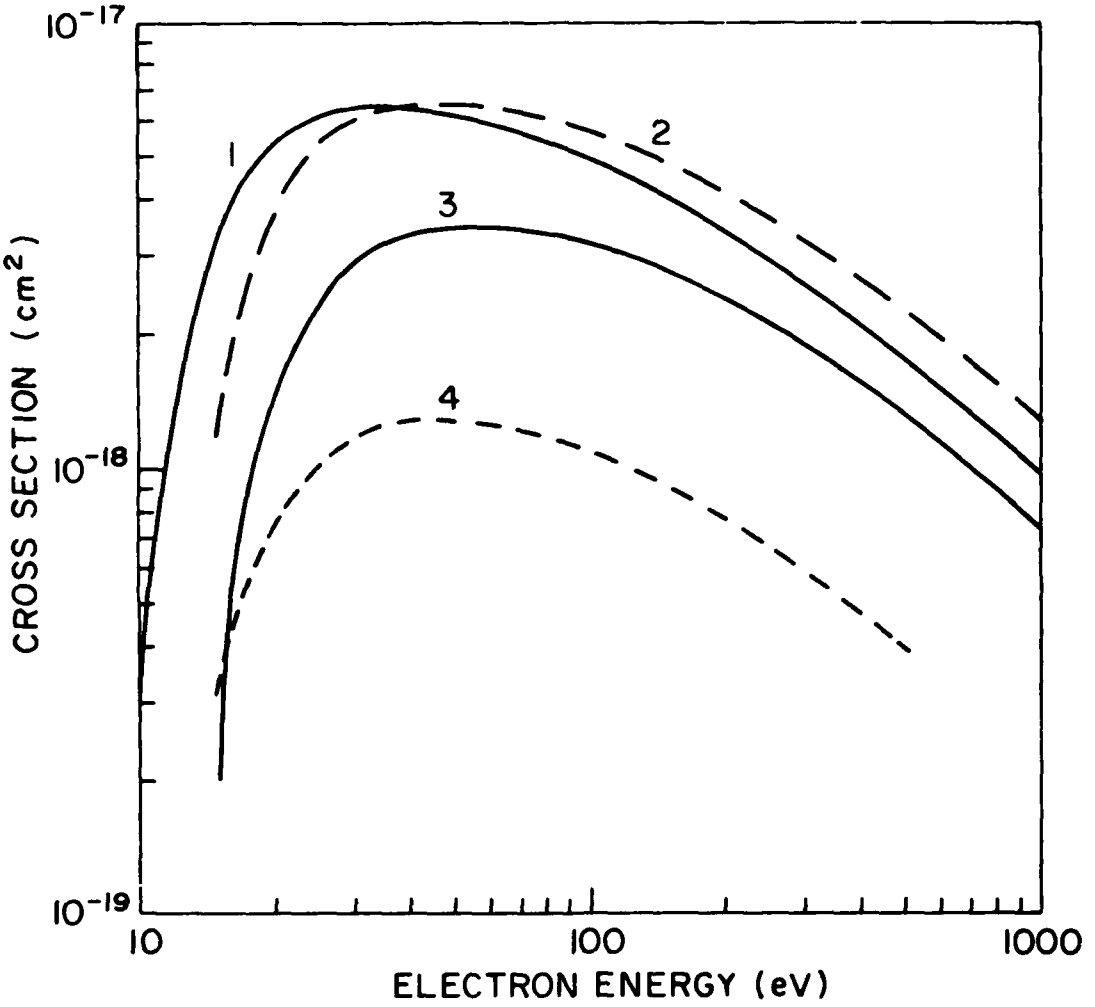

Fig. 29 — Electron impact excitation cross section for the optically allowed transitions in O. Curves 1, 2, 3 and 4 are for transition from ^3P to ^3S, $^3D^o$, $^3P^o$ and $^3D^o$ where excitation energies are 9.48, 12.48, 14.06 and 12.03 eV, respectively.

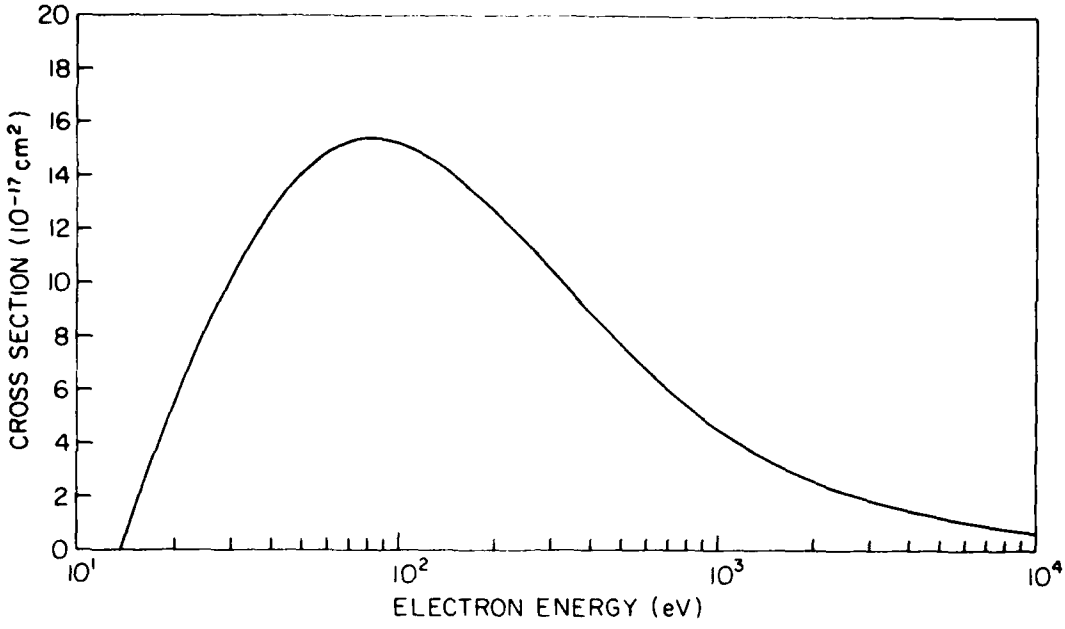

Fig. 30 — The electron impact ionization cross section of oxygen atom (ref. 53)

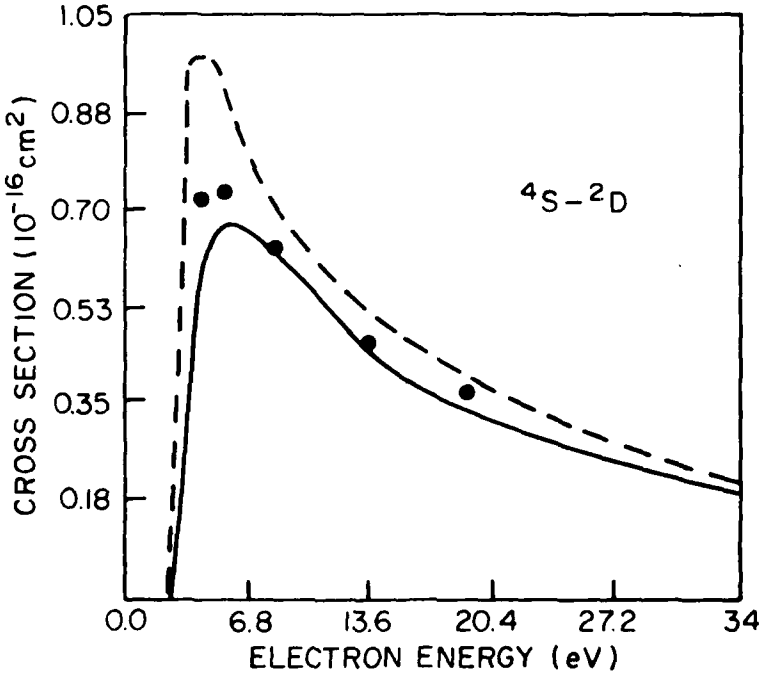

Fig. 31 — The electron impact excitation cross section for N(^{2}D). Solid curve (ref. 55), dashed curve (ref. 48) and circles (ref. 56).

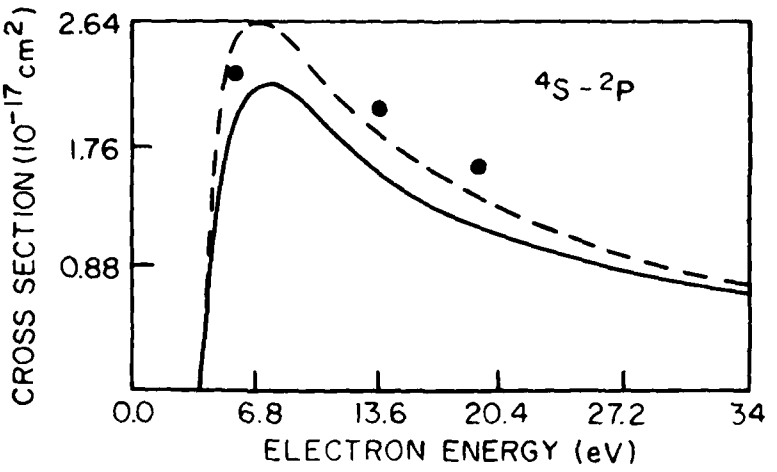

Fig. 32 — The electron impact excitation cross section of N(^{2}P). Solid curve, (ref. 55), cashed curve (ref. 48) and circles (ref. 56).

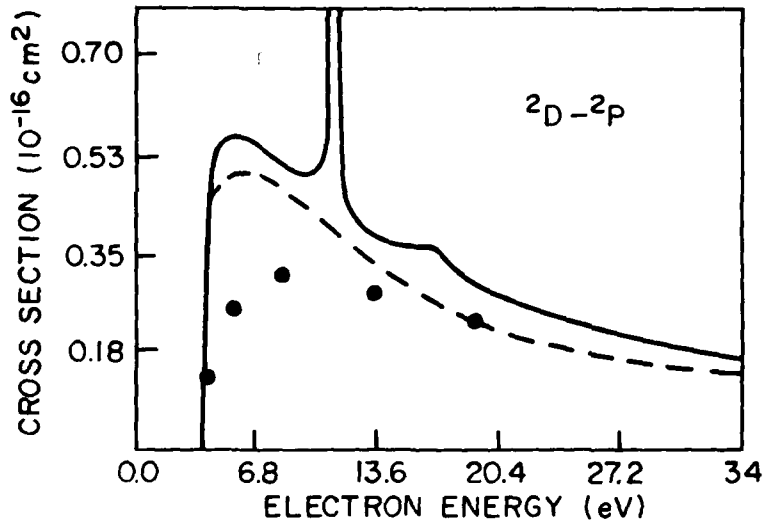

Fig. 33 — The electron impact excitation cross section for the ^{2}D-^{2}P transition in nitrogen. Solid curve (ref. 55), dashed curve (ref. 48) and circles (ref. 56).

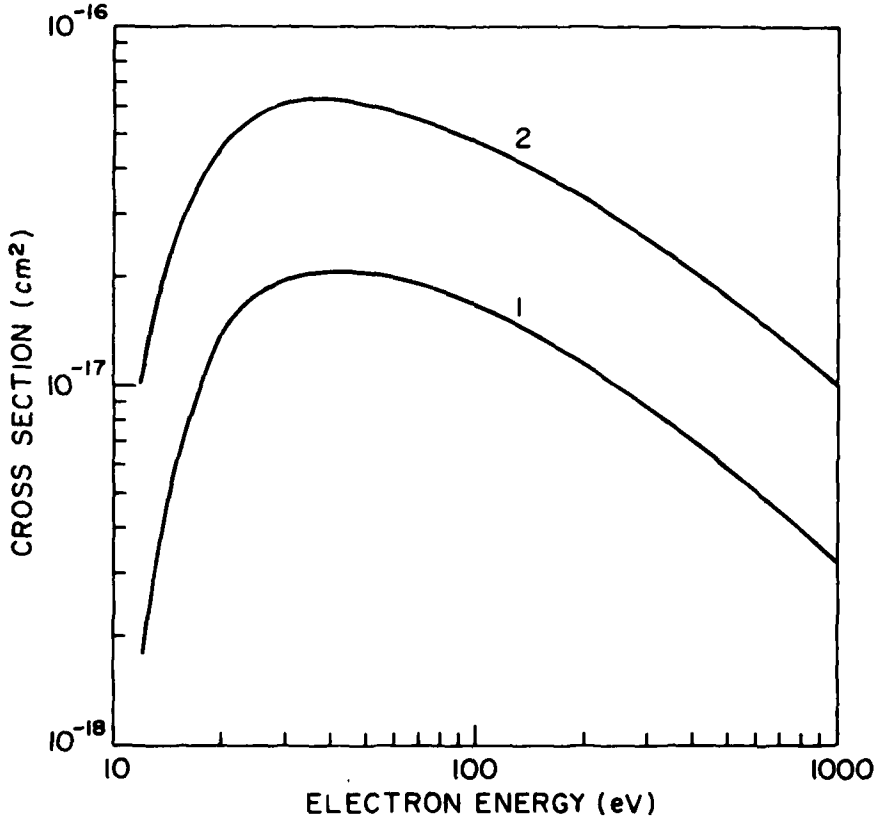

Fig. 34 — The electron impact excitation cross section for two optically allowed transitions in nitrogen, curve 1 for transitions $^4S^o$-^4P and $^4S^o$-^4P, where excitation energies are 10.87 and 10.28 eV, respectively.

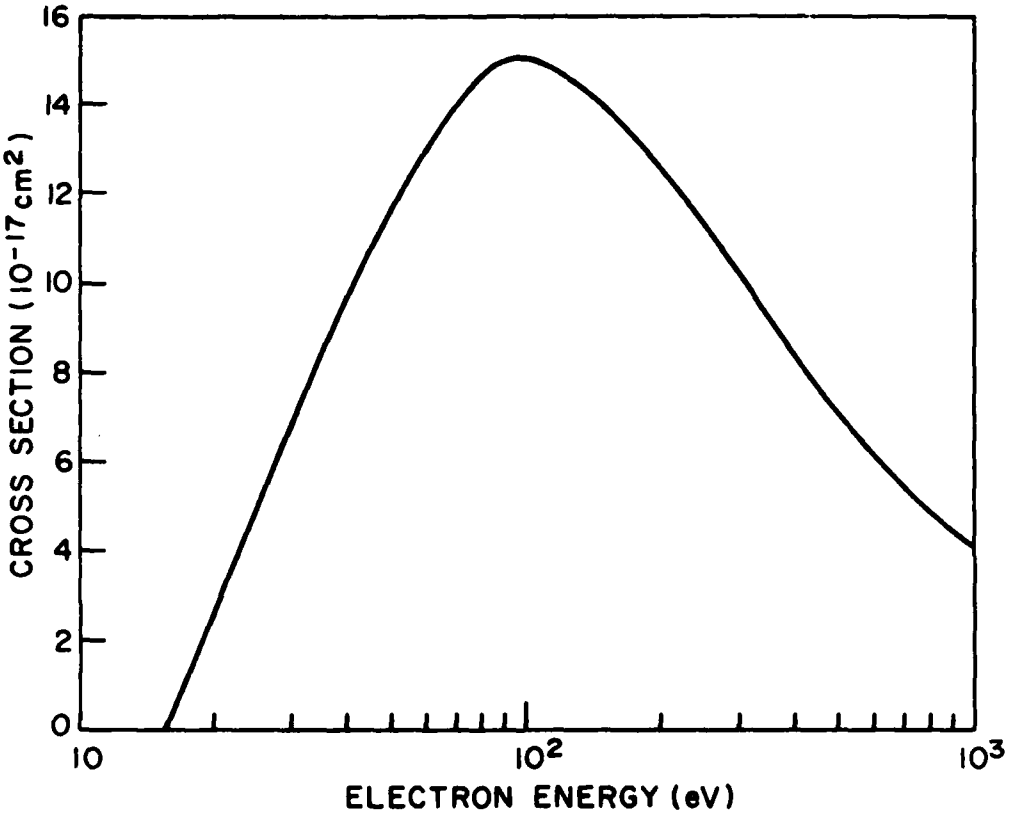

Fig. 35 — The electron impact ionization cross section for nitrogen atom (ref. 58)

REFERENCES

1. A. W. Ali and A. D. Anderson, "Low Energy Electron Impact Rate Coefficients for Some Atmospheric Species," NRL Report 7432, (1972).
2. G. J. Schulz, Phys. Rev. 135, A 988 (1964) and references therein.
3. H. Ehrhardt and R. Willman , Zeits, Phys. 204 462 (1967).
4. A. Herzenberg and F. Mandl Proc. Roy. Soc. (London) A270, 48 (1962).
5. J.C.Y. Chen, J. Chem. Phys. 40, 3507 (1964) and Phys. Rev. 146, 61 (1966).
6. D. T. Britwhistle and A. Herzenberg, J. Phys. B4, 153 (1971).
7. D. Spence, J. L. Mauer and G. J. Schulz, J. Chem. Phys. 57, 5516 (1972).
8. A. G. Engelhardt, A. V. Phelps and C. G. Risk, Phys. Rev. 135, A1566 (1964).
9. D. C. Cartwright, Aerospace Report #TR-0059(9260-01)-6, The Aerospace Corporation, El Segundo, CA. August (1970) and Phys. Rev. A2, 1331 (1970), Phys. Rev. A5, 1974 (1972).
10. S. Chung and C. C. Lin, Phys. Rev. A6, 988 (1972)
11. R. T. Brinkmann and S. Trajmar , Ann. Geophys.26, 201 (1970).
12. W. L. Borst, Phys. Rev. A5, 648 (1972).
13. D. C. Cartwright, S. Trajmar, A. Chutjian and W. Williams, Phys. Rev. A16, 1041 (1977).
14. V. I. Ochkur, Sov. Phys. JETP 18, 503 (1964).
15. M. R. H. Rudge, Proc. Phys. Soc. (London) 85, 607 (1965); 86, 763 (1965).
16. M. Imami and W. Borst, J. Chem. Phys. 61, 1115 (1974).
17. R. W. Nicholls, Annals de Geophys. 20, 144 (1964)
18. W. Benesch, J. T. Vanderslice, S. G. Tilford and P. G. Wilkerson, Astrophys. J. 143, 236 (1966).

19. T. G. Finn and J. P. Doering, J. Chem Phys. 64, 4490 (1976).

20. J. M. Ajello, J. Chem. Phys. 53, 1156 (1970)

21. A. Chutjian, D. C. Cartwright and S. Trajmar, Phys. Rev. A16, 1052 (1977).

22. H. F. Winters, J. Chem. Phys., 44. 1472 (1966).

23. E. C. Zipf and R. W. McLaughlin, Planet. Space Sci. 26. 449 (1978).

24. A. Niehaus, Z. Naturf. 22a, 690 (1967).

25. J. F. M. Aarts and F. J. deHeer, Physica 52, 45 (1971).

26. W. Sroka, Z. Naturf. 24a, 398 (1969).

27. J. M. Ajello, J. Chem. Phys. 53, 1156 (1970).

28. M. J. Mumma and E. C. Zipf, J. Chem Phys. 55, 5582 (1971).

29. D. Rapp and P. Englander-Golden, J. Chem. Phys. 43, 1464 (1965).

30. J. T. Tate and P. T. Smith, Phys. Rev. 39, 270 (1932).

31. D. Rapp, P. Englander-Golden and D. D. Briglia, J. Chem. Phys. 42, 4081 (1965).

32. G. R. Wight , M. J. Van der Wiel and C. E. Brion, J. Phys. B. Atom. Mol. Phys. 9, 675 (1976).

33. B. L. Schram, F. J. de Heer, M. J. Van der Weil and J. Kistemaker, Physica 31, 94 (1964).

34. M. N. Hirsch, P. N. Eisner, and J. A. Slevin, Phys. Rev. 178, 175 (1969).

35. W. L. Borst and E. C. Zipf, Phys. Rev. A1, 834 (1970).

36. W. R. Pendleton, Jr., and L. D. Weaver, Final Technical Report ARPA Order 1691, Contract F33657-71-C-0174, Advanced Research Project Agency 1973.

37. D. Spence and G. J. Schulz, Phys. Rev. A2, 1802 (1970).

38. F. Linder and H. Schmidt, Z. Naturf 26A, 1617 (1971)

39. S. Trajmar, D. C. Cartwright and W. Williams, Phys. Rev. A4, 1482 (1971).

40. S. Trajmar, W. Williams and A. Kuppermann, J. Chem. Phys. 56, 3759 (1972).

41. K. Wakiya, J. Phys. B. Atom. Mole. Phys. 11, 3931 (1978)

42. P. S. Julienne and M. Krauss, J. of Res. Nat. Bur. Stand. 76A, 661 (1972)

43. A. E. S. Green and R. S. Stolarski, J. Atom. Terr. Phys. 34, 1703 (1972).

44. K. Wakiya, J. Phys. B. Atom. Mole. Phys. 11, 3913 (1978).

45. C. C. Lin and S. Chung, AFGL-TR-78-0260 (1978)

46. J. W. McConkey and J. M. Woolsey, J. Phys. B. Atoms and Mol. Phys. 2, 529 (1969).

47. V. V. Skubenich, Soviet Optics and Spectroscopy 25, 190 (1968).

48. R. J. W. Henry, P. G. Burke and A. C. Sinfailam, Phys. Rev. 178, 218 (1969) and References therein.

49. L. D. Thomas and R. K. Nisbet, Phys. Rev. A11. 170 (1975).

50. Vo ky Lan, N. Feautrier, M. Le Dourneuf and Van Regemorter, J. Phys. B5, 1506 (1972).

51. H. W. Drawin, Report EUR-CEA-FC-383 Revised (1967).

52. E.J. Stone and E. C. Zipf, Phys. Rev. A4, 610 (1971). The results in this paper are modified as reported in T. Sawada, P. S. Ganas Phys. Rev. A7, 617 (1973).

53. W. L. Fite and R. T. Brackmann, Phys. Rev. A4, 610 (1971).

54. A. Dalgarno and G. Lejeune, Planet Space Sci. 19, 1653 (1971).

55. K. A. Berrington, P. G. Burke and W. D. Robb, J. Phys. B: Atom, Mol. Phys. 8, 2500 (1975).

56. S. Ormonde, K. Smith, B. W. Torress and A. R. Davies, Phys. Rev. A8, 262 (1973).

57. W. L. Wiese, M. Smith and B. M. Glennon, Atomic Transition Probabilities, Vol. I National Standard Reference Data System Report NSRDS-NBS-4 (1966).

58. A. C. Smith, E. Caplinger, R. H. Neynaber, E. W. Rothe and S. M. Trujillo, Phys. Rev. 127, 1647 (1962).

DISTRIBUTION LIST

Commander
Naval Sea Systems Command
Depart of the Navy
Washington, D.C. 20363
ATTN: NAVSEA 03H (Dr. C. F. Sharn)

Central Intelligence Agency
P.O. Box 1925
Washington, D.C. 20013
ATTN: Dr. C. Miller/OSI

Air Force Weapons Laboratory
Kirtland Air Force Base
Albuquerque, New Mexico 87117
ATTN: Maj. H. Dogliani
U.S. Army Ballistics Research Laboratory
Aberdeen Proving Ground, Marland 21005
ATTN: Dr. D. Eccleshall (DRXBR-BM)

Ballistic Missile Defense Advanced Technology Center
P.O. Box 1500
Huntsville, Alabama 35807
ATTN: Dr. L. Harvard (BMDSATC-1)

B-K Dynamics Inc.
15825 Shady Grove Road
Rockville, Maryland 20850
ATTN: Mr. I. Kuhn

Lawrence Livermore Laboratory
University of California
Livermore, California 94550
ATTN: Dr. R.J. Briggs
Dr. T. Fessenden
Dr. E.P. Lee
Dr. S. Yu
Mission Research Corporation
735 State Street
Santa Barbara, California 93102
ATTN: Dr. C. Longmire
Dr. N. Carron

National Bureau of Standards
Gaithersburg, Maryland 20760
ATTN: Dr. Mark Wilson

Science Applications, Inc.
Security Office
5 Palo Alto Square, Suite 200
Palo Alto, Calfornia 94304
ATTN: Dr. R.R. Johnston
Dr. Leon Feinstein

Naval Surface Weapons Center
White Oak Laboratory
Silver Spring, Maryland 20910
ATTN: Mr. R.J. Biegalski
Dr. R. Cawley
Dr. J.W. Forbes
Dr. D.L. Love
Dr. C.M. Huddleston
Mr. W.M. Hinckley
Dr. G.E. Hudson
Mr. G.J. Peters
Mr. N.E. Scofield
Dr. E.C. Whitman
Dr. M.H. Cha
Dr. H.S. Uhm
Dr. R.B. Fiorito

C.S. Draper Laboratories
Cambridge, Massachusetts 02139
ATTN: Dr. E. Olsson
Dr. L. Matson

Physical Dynamics, Inc.
P.O. Box 1883
Lajolla, California 92038
ATTN: Dr. K. Brueckner
Office of Naval Research
Department of the Navy
Arlington, Virginia 22217
ATTN: Dr. W.J. Condell (Code 421)
Dr. T. Berlincourt (Code 464)

Avco Everett Research Laboratory
2385 Revere Beach Pkwy.
Everett, Massachusetts 02149
ATTN: Dr. R. Patrick
Dr. Dennis Reilly

Defense Technical Information Center
Cameron Station
5010 Duke Street
Alexandria, VA 22314 (12 copies)

Naval Research Laboratory
Washington, D.C. 20375
ATTN: M. Lampe - Code 4792
M. Friedman - Code 4700.1
J.R. Greig - Code 4763 (50 copies)
I.M. Vitkovitsky - Code 4770
T. Coffey - Code 4000
Superintendent, Plasma Physics Division - Code 4700 (25 copies)
Library - Code 2628 (20 copies)
A. Ali - Code 4700.1T (25 copies)
J. Brown - Code 4701
V. Granatstien - Code 4740
R. Parker - Code 6805
T. Schriempf - Code 6330

Defense Advanced Research Projects Agency
1400 Wilson Blvd.
Arlington, Virginia 22209
ATTN: Dr. J. Mangano
Dr. J. Bayless

JAYCOR
205 S. Whiting St.
Alexandria, Virginia 22304
ATTN: Drs. D. Tidman
R. Hubbard
J. Gillory

JAYCOR
Naval Research Laboratory
Washington, D.C. 20375
ATTN: Dr. R. Fensler - Code 4770

Mission Research Corp.
1400 San Mateo, S.E.
Albuquerque, NM 87108
ATTN: Dr. Brendan Godfrey

Princeton University
Plasma Physica Laboratory
Princeton, NJ 08540
ATTN: Dr. F. Perkins, Jr.

McDonnell Douglas Research Laboratories
Dept. 223, Bldg, 33, Level 45
Box 516
St. Louis, MO 63166
ATTN: Dr. Michael Greenspan

Cornell University
Ithaca, NY 14853
ATTN: Prof. David Hammer

Sandia Laboratories
Albuquerque, NM 87185
ATTN: Dr. Bruce Miller
Dr. Barbara Epstein
Dr. John Olsen
Dr. Don Cook

Naval Air Systems Command
Washington, D.C. 20361
ATTN: Dr. R.J. Wasneski, Code AIR-350F

Beers Associates, Inc.
P.O. Box 2549
Reston, VA 22090
ATTN: Dr. Douglas Strickland

R and D Associates
P.O. Box 9695
Marina del Rey, California 90291
ATTN: Dr. F. Gilmore

Director
Defense Nuclear Agency
Washington, D.C. 20305
ATTN: Dr. C. Fitz (RAAE)
Dr. P. Lunn (RAAE)